

Categorization of Alzheimer's Disease stages using deep learning approaches with Mc Nemar's Test

Begüm Şener^{Corresp., 1}, Koray Acici², Emre Sümer³

¹ Department of Computer Engineering, Başkent University, Ankara, Başkent University, Ankara, Turkey

² Department of Artificial Intelligence and Data Engineering, Ankara University,, Ankara University, Ankara, Turkey

³ Department of Computer Engineering, Başkent University, Ankara, Baskent University, Ankara, Turkey

Corresponding Author: Begüm Şener

Email address: begume@baskent.edu.tr

Early diagnosis is crucial in Alzheimer's disease both clinically and for preventing the rapid progression of the disease. Early diagnosis with awareness studies of the disease is of great importance in terms of controlling the disease at an early stage. Additionally, early detection can reduce treatment costs associated with the disease. A study has been carried out on this subject to have the great importance of detecting Alzheimer's disease at a mild stage and being able to grade the disease correctly. This study's dataset consisting of MRI images from the Alzheimer's Disease Neuroimaging Initiative (ADNI) was split into training and testing sets, and deep learning-based approaches were used to obtain results. The dataset consists of three classes: Alzheimer's disease (AD), Cognitive Normal (CN), and Mild Cognitive Impairment (MCI). The achieved results showed an accuracy of 98.94% for CN vs. AD in the one versus one (1 vs. 1) classification with the EfficientNetB0 model and 99.58% for AD vs. CNMCI in the one versus All (1 vs. All) classification with AlexNet model. In addition, in the study, an accuracy of 98.42% was obtained with the EfficientNet121 model in MCI vs. CN classification. These results indicate the significant potential for mild stage Alzheimer's Disease detection of Alzheimer's disease. Early detection of the disease in the mild stage is a critical factor in preventing the progression of Alzheimer's disease. In addition, a variant of the non-parametric statistical Mc Nemar's Test was applied to determine the statistical significance of the results obtained in the study. Statistical significance of 1 vs. 1 and 1 vs. All classifications were obtained for EfficientNetB0, DenseNet, and AlexNet models.

1 **Categorization of Alzheimer's Disease Stages Using** 2 **Deep Learning Approaches and McNemar's Test**

3 Begüm Şener¹, Koray Açııcı², Emre Sümer³

4 ¹ Department of Computer Engineering, Başkent University, Ankara, Turkey

5 ² Department of Artificial Intelligence and Data Engineering, Ankara University, Ankara, Turkey

6 ³ Department of Computer Engineering, Başkent University, Ankara, Turkey

7

8 Corresponding Author:

9 Begüm Şener¹

10 Fatih Sultan Street Baglica Campus, Etimesgut/Ankara, 06790, Turkey

11 Email address: begume@baskent.edu.tr

12

13 **ABSTRACT**

14 Early diagnosis is crucial in Alzheimer's disease (AD), both clinically and for the prevention of
15 rapid disease progression. Studies focused on early diagnosis based on disease awareness are of
16 great importance in terms of disease control at an early stage. Additionally, early diagnosis reduces
17 treatment costs. A recent study has drawn attention to the significance of detecting AD at a mild
18 stage and the ability to correct disease grading. This study's dataset consists of magnetic resonance
19 imaging (MRI) images from the Alzheimer's Disease Neuroimaging Initiative (ADNI), which are
20 split into training and testing sets. Deep learning-based approaches were used to obtain the study
21 results. In addition, a variant of the nonparametric statistical McNemar's test was applied to
22 determine the statistical significance of the results obtained in the study. The statistical significance
23 of one-versus-one and one-versus-all classifications was obtained for the EfficientNetB0,
24 DenseNet, and AlexNet models. The dataset consists of three classes: AD, cognitive normal (CN),
25 and mild cognitive impairment (MCI). The achieved results showed an accuracy of 98.94% for
26 CN vs. AD in the one-versus-one classification with the EfficientNetB0 model and 99.58% for
27 AD vs. CNMCI in the one-versus-all classification with the AlexNet model. In addition, an
28 accuracy of 98.42% was obtained with the EfficientNet121 model in MCI vs. CN classification in
29 our study. These results reveal the significant potential of deep-learning methodology for mild-
30 stage AD detection.

31 **Subjects:** Classification of Alzheimer's Disease, Diagnosis

32 **Keywords:** Alzheimer's disease, deep learning, classification, early diagnosis, McNemar's test

33 **INTRODUCTION**

34 Alzheimer's disease (AD), a common type of dementia, is a neurological disease that destroys
35 brain cells, reduces cognitive function, and occurs as a result of the accumulation of toxic proteins
36 in some parts of the brain. Symptoms of this disease appear gradually with age. The disease, which
37 begins with simple forgetfulness in the initial stage, can progress to symptoms such as the patient

38 forgetting events in their own recent past and losing the ability to recognize their immediate
39 environment and family members as time progresses. In the later stages of the disease, it may be
40 challenging to meet the patient's basic needs and provide care (Cummings & Cole 2002).

41 Detecting AD at an early stage is both clinically crucial and valuable for preventing the rapid
42 progression of the disease. Studies focusing on early diagnosis based on disease awareness are
43 important for controlling the disease at an early stage. While this situation improves the quality of
44 life both for the patients and their relatives, it also reduces the treatment costs of the disease.
45 Several imaging techniques have been associated with diagnosing AD (Colligris et al. 2018). AD
46 progresses through three stages (Hart et al. 2003). The early stage typically lasts 2 to 4 years.
47 During this stage, individuals experience frequent short-term memory problems, repetitions in
48 speech and questions, mild difficulties in self-expression, difficulties in writing and using objects,
49 the development of depression, personality changes, the inability to learn new skills, denial of the
50 disease, and irritability. During the middle stage, the patient might experience progressive memory
51 impairments, disturbances in orientation, difficulties in establishing cause-effect relationships,
52 sleep disorders, and an inability to acquire new information. In the advanced stage, the patient
53 might experience confusion between the past and present, severe impairment in communication,
54 falls, bed dependency, swallowing problems, pronounced psychiatric symptoms, and being
55 entirely in need of care.

56 The radiological approaches used for the diagnosis of AD include computed tomography (CT),
57 magnetic resonance imaging (MRI), functional MRI (fMRI), positron emission tomography
58 (PET), and single-photon emission computed tomography (SPECT). These are standard
59 procedures for diagnosis. In MRI, three separate images of the same region are available, each
60 with different tissue contrast: T1-weighted, T2-weighted, and proton-weighted images (Buxton et
61 al. 1987). Water appears black on T1-weighted images, white on T2-weighted images, and gray
62 on proton-weighted images. Because there were few uses of proton-weighted images, these images
63 were removed from standard reviews.

64 The inspiration for studying this problem was found during the examination of other studies in
65 the literature. These studies found that advanced-stage AD can be detected relatively easily,
66 whereas mild-stage AD is more difficult to detect. The necessity and significance of detecting AD
67 in the mild stage is the reason for conducting this study.

68 The main aims of the study are as follows:

- 69 • Demonstrate the performance of deep learning models in the diagnosis of AD during the
70 middle stage of the disease.
- 71 • Show the effects of classifying classes in models as one-versus-one or one-versus-all.
- 72 • Overcome the difficulties in identifying patients with cognitive normal (CN) and mild
73 cognitive impairment (MCI) and detect AD at the mild stage before it progresses.

74 The manuscript is structured as follows: First, we briefly describe AD. Afterward, deep learning
75 techniques and the literature on AD are presented as an overview. After defining the dataset, the
76 methodology is presented. The methodology section provides definitions and evaluation metrics

77 of the models used. Finally, we discuss the results obtained and present our conclusions, including
78 recommendations for future work.

79
80

81 **RELATED WORK**

82 There are numerous studies in the literature on the diagnosis of AD. A summary of the literature
83 review on AD is presented in the following section.

84 Mora-Rubio et al. (2023) presented a deep learning-based approach to classifying MRI scans at
85 different stages of AD using a set of images compiled from the Alzheimer's Disease Neuroimaging
86 Initiative (ADNI) and Open Access Series of Imaging Studies (OASIS). They used data
87 augmentation operations such as preprocessing, rotation, translation, and zooming using
88 FreeSurfer. They obtained results using state-of-the-art convolutional neural networks (CNNs)
89 such as EfficientNet and DenseNet. The best results obtained were 89% for CN vs. AD, 80% for
90 CN vs. late MCI (LMCI), 66% for CN vs. MCI, and 67% for CN vs. early MCI (EMCI).

91 Shanmugam et al. (2022) utilized the ADNI dataset to work on five classes: CN, EMCI, MCI,
92 LMCI, and AD. Using a total of 7800 images, they divided the image data of the five classes into
93 60% for training, 20% for testing, and 20% for validation. The results were obtained over 100
94 epochs. The images were adjusted to the required dimensions for processing through the respective
95 models. Using transfer learning, the study proposed three different deep learning models, namely
96 AlexNet, ResNet-18, and GoogLeNet. According to the results, the AlexNet model achieved an
97 accuracy of 97.34% for CN, 97.51% for EMCI, 95.19% for LMCI, 96.82% for MCI, and 94.08%
98 for AD. The ResNet-18 model achieved an accuracy of 98.88% for CN, 99.14% for EMCI, 98.88%
99 for LMCI, 98.71% for MCI, and 97.51% for AD. The GoogLeNet model achieved an accuracy of
100 97.17% for CN, 98.28% for EMCI, 97.60% for LMCI, 98.37% for MCI, and 96.39% for AD. The
101 authors are planning future work focused on designing deep learning networks specifically for
102 classifying AD cases.

103 In the study by Mehmood et al. (2021), T1-weighted MRI images from 300 AD patients in the
104 ADNI dataset were used. Their proposed transfer learning model divided the layers into two
105 groups, gradually training some layers while freezing the remaining ones. In the recommended
106 neural network models, Group A had three max-pooling convolutional layers, while Group B had
107 four max-pooling convolutional layers, which were frozen. They used six binary classifications
108 and evaluated the performance of their proposed transfer learning model: CN vs. EMCI, CN vs.
109 AD, CN vs. LCMI, EMCI vs. LMCI, EMCI vs. AD, and LMCI vs. AD. They evaluated the models
110 with and without data augmentation. The data were divided into 80% for training and 20% for
111 testing. They also used some of the 20% test MRI images for validation. For Group A, the highest
112 accuracy without data augmentation was achieved in comparing CN vs. AD, with an accuracy of
113 93.83%. With data augmentation, the highest accuracy in the CN vs. AD comparison reached
114 95.38%. For Group B, the highest accuracy without data augmentation was achieved in comparing
115 CN vs. AD, with an accuracy of 95.33%. With data augmentation, the highest accuracy in the CN
116 vs. AD comparison reached 98.73%.

117 Mohammadjafari et al. (2021) experimented with CNN methods using the OASIS and ADNI
118 AD datasets. They utilized the ADNI-1 dataset, which consists of 95 MRI scans of AD patients
119 and 113 MRI scans of healthy individuals (CN). The images were resized to 224×224 and
120 converted to red, green, and blue (RGB) bands to fit the training configurations models. They used
121 5-fold cross-validation to validate the models. They obtained average accuracy for the baseline
122 model, transfer learning with the baseline model, and transfer learning with the ProtoPNet model.
123 For the baseline model, they achieved an accuracy of 75.76% for VGG-16, 77.06% for ResNet50,
124 and 73.23% for DenseNet121. When performing transfer learning with the ProtoPNet model, the
125 observed accuracies were 71.70% for VGG-16, 90.30% for ResNet50, and 91.02% for
126 DenseNet121.

127 Sethi et al. (2022) utilized the ADNI dataset to conduct a study on the MRI images of 50 patients
128 for each class (AD, CN, and MCI). They used 80% of the dataset for training and 20% for model
129 testing. They used 23,232 images for training and 6468 images for testing. They achieved results
130 by combining CNN with support vector machines (SVM) as a hybrid model. When only the CNN
131 model was used, the highest accuracy rate was 82.32% for CN vs. AD, and the test accuracy rate
132 was 85.1%. When the hybrid model of CNN and SVM was used, the highest accuracy rate was
133 again 89.4% for CN vs. AD, and the test accuracy rate was 88%.

134 Naz et al. (2021) studied T1-weighted MRI images using the ADNI dataset. They evaluated 11
135 pretrained CNN models. They extracted features from FC CNN layers and studied the MCI-AD,
136 AD-CN, and MCI-CN classes. The dataset contained 95 AD, 95 CN, and 146 MCI. Each patient
137 had a different number of scans, ranging from a minimum of three to a maximum of 15. Digital
138 Imaging and Communications in Medicine (DICOM) images were converted to Joint Photographic
139 Experts Group (JPEG) format. By augmenting the dataset, they obtained 37,590 images after
140 augmentation, whereas the original dataset had 3925 images. They divided the dataset into 80%
141 for training, 10% for testing, and 10% for validation. Using the frozen features extracted from the
142 augmented dataset and the VGG-19 model, they achieved the highest accuracy rate of 99.27% for
143 MCI vs. AD. The VGG-16 model obtained an accuracy rate of 98.89% for CN vs. AD and 97.06%
144 for CN vs. MCI. Using the AlexNet model, they obtained an accuracy rate of 91.38% for CN vs.
145 AD.

146 In their study, Farooq et al. (2017) used the ADNI dataset of 149 AD patients. They divided the
147 dataset into 33 AD, 22 LMCI, 49 MCI, and 45 CN as 75% training and 25% testing and used 10%
148 of the training set for validation. To eliminate the imbalance in each class in the dataset, they used
149 38,024 images by increasing the number of images of the missing classes. They obtained an
150 average accuracy of 98.88% for the AlexNet model, an average accuracy of 98.01% for ResNet-
151 18, and an average accuracy of 98.14% for ResNet-152.

152 The study by Savaş (2022) used T1-weighted and sagittal images in the ADNI-1 dataset. There
153 were 382 patients in the dataset, of which 223 were male and 159 were female. The dataset was
154 split into 90% for training and 10% for testing, and 10% of the 90% training portion was used for
155 validation. Images were resized to 224×224 . The dataset has three classes: 135 CN images, 148
156 MCI images, and 99 AD images. Deep neural network architectures created using the CNN

157 algorithm were used to analyze the data employed in the study. Models other than the ResNet
158 model were set to run for 250 epochs because the learning increment in the other models continued.
159 In the test results of the model, EfficientNetB0 provided the best result, with 92.98%, followed by
160 EfficientNetB1, with 91.91%. The lowest accuracy rate was 77.40% with the Xception model. The
161 AD sensitivity value for EfficientNetB0 was 94.34%, the sensitivity value for MCI was 94.25%,
162 and the sensitivity value for CN was 86.17%. The specificity value, on the other hand, was 96.96%
163 for CN at the highest rate.

164 Li et al. (2017) conducted a study that utilized T1-weighted sagittal MRI images from the ADNI
165 dataset. There are 427 AD patients in the dataset, of which 199 have AD and 229 are healthy (CN).
166 They used 5-fold cross-validation to evaluate classification performance and to train and test
167 models. First, they obtained the results for the individual models they proposed, and then they
168 obtained results by combining these models. They used MRI images sized $69 \times 59 \times 57$ for
169 CNN_S3, $102 \times 88 \times 85$ for CAE_S2, $69 \times 59 \times 57$ for CAE_S3, and $54 \times 44 \times 43$ for CAE_S4.
170 They achieved 84.12% accuracy for the CNN_S3 model, 82.24% for the CAE_S2 model, 81.19%
171 for the CAE_S3 model, 76.17% for the CAE_S4 model, and 88.31% accuracy with all of the
172 models combined.

173 In their study, Khan et al. (2022) used the ADNI dataset divided into 70% for training and 30%
174 for testing. The dataset contained 2127 images that were axial and T1- and T2-weighted. Their
175 data included 612 AD, 538 MCI, and 975 CN classes. To ensure the highest pixel quality, the
176 images were resized to dimensions of 512×512 . Afterward, the images were standardized and
177 normalized. They obtained results using extreme gradient boosting (XGB), decision trees (DTs),
178 and decision support machines. They achieved an accuracy of 89.77% in the XGB + DT + SVM
179 hybrid model. Subsequently, all models' efficiency was optimized using grid-based tuning, and
180 they saw a significant improvement in the results obtained after this process. The best average
181 accuracy rate was 95.75% due to the optimized parameters. They achieved an accuracy rate of
182 96.12% for the AD class, 95% for the CN class, and 96.15% for the MCI class.

183 Mohi ud din dar et al. (2023) studied the ADNI dataset using T2-weighted MRI images. The
184 dataset included data from 300 AD patients divided into five classes: CN, MCI, EMCI, LMCI, and
185 AD. There were 1101 images in the LMCI class, 493 in the AD class, 204 in the EMCI class, 61
186 in the LMCI class, 198 in the MCI class, and 493 in the CN class. They resized all the images to
187 224×224 and processed RGB images using three channels. Because of the dataset's instability,
188 the insufficient data were multiplied by the data augmentation method in the form of 580 MRI
189 images for each class. The dataset was balanced, and a total of 2900 images were processed. In the
190 enhancement method, some techniques, such as horizontal flip and 5-degree rotation, were used
191 in the images. They divided the dataset into 80% for training, 10% for testing, and 10% for
192 validation. The images were normalized during preprocessing. Using the CNN architecture, the
193 researchers achieved an average accuracy rate of 96.22% after training for 100 epochs.

194 Islam & Zhang (2017) used the OASIS dataset in their study. They performed classification
195 using T1-weighted MRI scans of the OASIS dataset, which comprised four classes and 416
196 subjects. They used the Inception-v4 model to create a framework with suggestions. The 5-fold

197 cross-validation method was preferred while running the model. The results were obtained by
198 running the model for both five and 10 epochs; the researchers obtained an accuracy rate of 71.25%
199 after training for five epochs and 73.75% after training for 10 epochs.

200 Mamun et al. (2022) obtained the dataset for their study online via Kaggle. It comprised 6219
201 MRI images with four classes. After the dataset was preprocessed by resizing images, removing
202 noises, segmenting images, and performing smoothing operations, the dataset was trained using
203 the holdout cross-validation method. They obtained results using a proposed CNN architecture,
204 and the highest accuracy rate they achieved was 97.60%. In addition, other metrics, such as AUC,
205 recall, and loss values, were given along with the statistical analysis comments.

206 Sekhar & Jagadev (2023) used an AD MRI preprocessed dataset in their study. The dataset
207 comprised 6400 MRI images with four classes. The dataset was divided into train, test, and
208 validation portions. The researchers found that the advantage of end-to-end learning was that it
209 could create an effective visual explanation of the logic behind the classification results obtained
210 using CNN, which will help medical experts understand the impact of CNN and find new
211 biomarkers. The best result they obtained was 98.5% with the EfficientNet model.

212 A summary of the literature is provided in Table 1.

213

Table 1. Summary of the studies.

214 To summarize, the studies reviewed in this paper present the most commonly proposed models
215 and innovations in classifying AD using deep learning techniques. In addition to the one-versus-
216 one classification, we also present the results obtained from the one-versus-all classification, an
217 approach that has been less common in AD research. In the next sections, we present a study
218 performed using a different, more recent dataset and explore the potential changes in model
219 performance.

220 DATASET

221 The ADNI dataset, which was obtained from the ADNI database (accessible via the website
222 <http://adni.loni.usc.edu>), was employed in this study. Launched in 2016, the ADNI-3 dataset aims
223 to comprehensively identify relationships between clinical, genetic, imaging, cognitive, and
224 biochemical biomarker features across the entire spectrum of AD. ADNI-3 also includes brain
225 scans that detect tau protein tangles (tau PET), a crucial disease indicator. The ADNI datasets were
226 analyzed for AD detection. Because we found that the most recent data were in the ADNI-3 dataset,
227 our analysis studies were started using the ADNI-3 dataset.

228 In this study, T1-weighted structural MRI data and axial brain slices from the ADNI-3 dataset
229 were used for 515 AD patients, including 40 AD, 140 MCI, and 335 CN patients. Multiple scans
230 of each subject were taken at different times, and each subject had a different number of scans.
231 There were 259 female and 256 male individuals in the dataset. The dataset included data that were
232 last released in November 2022. Because of the unbalanced class distributions in the dataset, it
233 was arranged to balance the number of brain scans in each class. The Python programming
234 language was used to conduct these analyses.

235 Individuals with AD had received an AD diagnosis before the beginning of the study period.
236 CN subjects were in good health from the beginning of the study period and maintained good
237 health throughout the study. MCI subjects had begun to show symptoms of AD by the beginning
238 of the study period but had not yet fully progressed to AD and were not as healthy as the CN
239 subjects. Table 2 presents the classes, number of subjects, and total scan numbers of the classes.

240 Table 2. Classes and total scan numbers of these classes are given.

241 The image data format of the images in the dataset was Neuroimaging Informatics Technology
242 Initiative (NIFTI), which has a file extension of .nii. These image files were converted to portable
243 network graphic (PNG) images. During data preprocessing, each input MRI image in our CNN
244 model was resized to 224×224 before it was fed into the model because the model architectures
245 used 224×224 input images.

246

247 **METHODOLOGY**

248 **Convolutional Neural Network**

249 The CNN model's architecture consists of five convolution blocks, pooling layers, and a fully
250 connected (FC) layer. FC layers are used to calculate the output of each input MRI image. In the
251 FC layer, the image that passes through the convolutional and pooling layers several times and is
252 in the form of a matrix is transformed into a flat vector.

253 The labeling process was initiated after data collection, image resizing, and the conversion of
254 NIFTI images to PNG format. The label classes from the images and the comma-separated values
255 (CSV) file were mapped to each other. In the next step, the dataset was divided into 70% for
256 training and 30% for testing. A total of 10% of the 70% training portion was selected as the
257 validation set and was used during the data evaluation process.

258 The EfficientNetB0, DenseNet121, and AlexNet CNN models were applied to MRI images
259 using TensorFlow (TensorFlow, 2023) and Keras (Costa, 2023) applications. When we selected
260 the models, the importance of each model was taken into consideration. AlexNet and DenseNet121
261 models have shown that CNNs have revolutionized image processing. The AlexNet model has a
262 relatively simple design, which makes it relatively easy to train and implement. This is important
263 for applications in which time and cost are essential, such as AD classification. Because of its
264 impressive performance, simplicity, and generality, the AlexNet model was chosen; we believed
265 that it would provide significant advantages for this application. Because the EfficientNetB0 model
266 is a CNN model that shows impressive results in terms of scalability and performance, it can
267 achieve high accuracy and performance in classification tasks using fewer parameters and less
268 computational power. Because of these important and powerful features, we preferred to use the
269 EfficientNetB0 model over the other models.

270 While running the models, the relationship between the values obtained in each epoch was
271 observed and care was taken to avoid overfitting. The optimization of CNN models using the
272 dropout process is an important step to improve the performance of the models by preventing

273 overfitting. Thus, the dropout process was performed for the three models used. The dropout
274 process also increases the learning capacity of the models, making them more robust. Pooling was
275 also conducted for each model, which helped the model train faster and reduced the computational
276 power required by shrinking the images. We also investigated the rationale behind avoiding
277 traditional machine learning models such as XGBoost or LightGBM. Although these models are
278 effective in many situations, difficulties in terms of memory utilization and computational power
279 can be encountered when working with large datasets. The symptoms of AD can be complex and
280 multifaceted, and the reliability of models for medical diagnostics is therefore critical. Models
281 such as LightGBM or XGBoost may have limitations in accurately capturing this complexity.

282 **Convolutional Layer**

283 The convolutional layer is an artificial neural network layer that is a fundamental component of
284 deep learning and feature extraction. These layers are structures in which successful results can be
285 obtained, especially in the use cases of image processing and pattern recognition. The convolution
286 process is applied to the input data. It can create multiple feature maps using many different filters.
287 Convolutional layers are often used with activation functions (rectified linear unit [ReLU]) and
288 sequentially applied to convolution, pooling, and subsampling layers (Albawi et al. 2017).

289 **Pooling Layer**

290 Pooling layers are a type of layer used in CNN models. Pooling layers can be used to reduce
291 data size; they can also merge feature maps and protect critical information. The two most
292 commonly used pooling methods are maximum pooling and average pooling. Maximum pooling
293 creates a summary of the region by selecting the highest feature value within each region to
294 preserve its most important features and maintain its originality. Average pooling summarizes the
295 region by averaging the feature values within each region. This method reduces noise and provides
296 a smoother summary of the features. Pooling layers are usually used after many convolutional
297 layers, thus reducing the size of feature maps and summarizing the output data. Pooling layers help
298 deep learning models learn more general and high-level features and increase the network's
299 generalization ability (Sun et al. 2017).

300 **Fully Connected Layer**

301 The FC layer is an artificial neural network layer, also known as a densely connected layer. It
302 receives the outputs of all units (neurons) in the previous layer and connects each output with its
303 neurons. It can be the last layer of a neural network model (to provide an output such as
304 classification or regression), or it can be used in the middle layers of the model. FC layers are
305 widely used in deep learning models. These usually contain a large number of neurons and increase
306 the learning capacity of the model. These layers are often combined with activation functions
307 (ReLU, sigmoid, etc.) to add nonlinearity to the inputs. In summary, the FC layer is a neural
308 network layer that connects the input vector to all output units, increases the learning capacity of
309 the neural network, and helps the model learn complex relationships (Basha et al. 2020).

310 **Softmax Classification Layer**

311 The Softmax classification layer is an output layer used to address classification problems in
312 artificial neural network models. This layer transforms a model's inputs into an output vector
313 representing probabilities that can be assigned to classes. Using the Softmax function, this layer
314 transforms the network's outputs into class probabilities. The input vector values reaching the layer
315 are initially processed by the Softmax function. The Softmax function converts the input values
316 into probability values to calculate the value of each output unit. This transformation provides a
317 probability distribution in which the sum of all output units equals 1 (Maharjan et al. 2020).

318 **EfficientNetB0**

319 EfficientNetB0 is a widely used image classification model in deep learning. EfficientNet is a
320 family of models developed by Google Brain and optimized for scalability, efficiency, and
321 performance. B0 represents the lowest value of the scaling coefficient of the model.
322 EfficientNetB0 is an optimized model designed for high-performance image classification
323 problems using the CNN's powerful features. The model's features and performance have been
324 carefully designed with scaling strategies such as weight sharing, depth scaling, and width scaling.
325 Because of this, although it is a lighter model, it can provide similar or better performance than
326 other larger and more complex models. It is a model that is generally preferred for use on small
327 and medium-sized datasets. However, higher-scale EfficientNet (B1, B2, B3, ...) models are also
328 available for larger, more complex datasets and more demanding tasks (Marques et al. 2020).

329 **DenseNet121**

330 DenseNet is a family of models based on the concept of dense connections. DenseNet121 is a
331 widely used image classification deep learning model that is a member of this model family and
332 consists of 121 layers. The model's name refers to the number of layers in which dense connections
333 are used. The DenseNet structure, unlike traditional CNNs, uses dense connections in each layer
334 in which the outputs of all previous layers are used as inputs. These dense connections facilitate
335 the flow of information by combining the previous layer's outputs with the next layer's inputs. In
336 this way, each layer can access the outputs of all previous layers. Dense connections improve the
337 effectiveness and efficiency of information and mitigate the gradient loss problem regardless of
338 the depth of the network. DenseNet121 improves performance by combining the power of CNNs
339 with dense connections. This model is generally preferred for use on medium-sized datasets.
340 Trained on the ImageNet dataset, DenseNet121 is tailored for tasks such as image classification.
341 This model has been used successfully in many deep learning projects and image analysis
342 applications (Solano-Rojas et al. 2020).

343 **AlexNet**

344 AlexNet represents a significant milestone within deep learning and CNNs and is an artificial
345 neural network model of paramount importance. It was developed in 2012 by Alex Krizhevsky,
346 Geoffrey Hinton, and Ilya Sutskever and features a much deeper structure than those of other

347 models from that period. It contains eight layers, five of which are convolutional layers and two
348 of which are FC consecutive layers. AlexNet pioneered the widespread use of CNNs and made a
349 significant impact on the field of deep learning (Omonigho et al. 2020).

350 **One-Versus-One Classification**

351 One-versus-one is a method that treats multiclass classification problems as pairwise
352 comparisons between two classes. A separate classifier is created for both classes, and a pair of
353 classifiers is created for each class combination. For example, if you have a total of N classes, the
354 one-versus-one method creates a total of $(N \times (N - 1)) / 2$ classifiers. The one-versus-one method
355 increases the ease and speed of solving each binary classification problem. It also allows for the
356 use of more common binary classification algorithms as multiclass classification algorithms,
357 transforming multiclass classification into binary classification (Lingras & Butz 2007).

358 **One-Versus-All Classification**

359 One-versus-all is a method that treats multiclass classification problems as one class, which
360 distinguishes each class from the others, as well as all remaining classes. This method aims to
361 solve multiclass classification problems by transforming them into binary classification problems.
362 In the one-versus-all method, a separate classifier (for example, a binary classifier or binary
363 classification model) is created for each class. When a separate classifier is created for each class,
364 this classifier is trained to distinguish that class from other classes. In contrast, all remaining
365 classes are combined to form a single “other” class. The one-versus-all method requires as many
366 classifiers as there are classes. The advantage is that binary classification algorithms can be used,
367 and each class can be learned separately. This provides a more flexible solution when class labels
368 are unstable or the complexity is different between classes (Lingras & Butz 2007).

369 **Performance Evaluation Metrics**

370 Various metrics are used to evaluate the performance of models. Accuracy provides an overview
371 of the prediction quality and indicates the proportion of correctly classified samples. On the other
372 hand, precision indicates the proportion of true positive predictions among the values we predicted
373 as positive. Sensitivity (recall) is a metric that demonstrates the proportion of positive instances
374 correctly predicted among the actual positive instances. The F1 score is a performance metric that
375 aims to strike a balance between precision and sensitivity and is calculated by using the harmonic
376 mean. The area under the curve (AUC) represents the area under the receiver operating
377 characteristic (ROC) curve. AUC measures the performance of the classification model with a
378 single numerical value. From 0 to 1, the AUC value signifies superior model performance as it
379 approaches higher values. The Matthews correlation coefficient (MCC) is used in binary
380 classification problems and measures the correlation of classification results with actual classes.
381 The MCC is computed on the basis of true positives, true negatives, false positives, and false
382 negatives. The MCC takes a value between -1 and $+1$. A value of $+1$ represents excellent
383 forecasting performance, whereas -1 represents completely inverse forecasting performance. A
384 value of 0 represents the same performance as randomly guessing. The MCC is a widely used

385 performance evaluation metric, especially in medical diagnostics, bioinformatics, and genetic
386 research. The metrics are computed using Equations (1) to (5).

$$387 \quad \text{Accuracy} = \frac{TP + TN}{TP + TN + FP + FN} \quad (1)$$

$$388 \quad \text{Precision} = \frac{TP}{TP + FP} \quad (2)$$

$$391 \quad \text{Recall} = \frac{TP}{TP + FN} \quad (3)$$

$$392 \quad \text{F1 Score} = \frac{2 * \text{Precision} * \text{Recall}}{\text{Precision} + \text{Recall}} \quad (4)$$

$$396 \quad \text{MCC} = \frac{TP * TN - FP * FN}{\sqrt{(TP + FN) * (TP + FP) * (TN + FP) * (TN + FN)}} \quad (5)$$

399 The equations' components include true positive (TP), true negative (TN), false positive (FP),
400 and false negative (FN). The experiments in this study utilized NVIDIA graphics processing unit
401 (GPU) resources using Google Colab. These GPUs provide a considerable advantage in
402 computationally intensive operations such as deep learning. In the study, the results were obtained
403 using the T4 GPU.

404 McNemar's Test

405 McNemar's test is widely used, especially in comparing the performance of classification
406 algorithms. It is commonly used when comparing the performance of two classification or
407 diagnostic tests on the same dataset. McNemar's test assesses whether the difference between these
408 discordant pairs is statistically significant and is used to determine if there is a change or
409 improvement in performance between two tests. It is often used in medical research to compare
410 the effectiveness of different diagnostic methods or treatments (Bostanci & Bostanci 2012). The
411 methodology of the research is presented in Fig. 1.

412  Figure 1. Research methodology.

413 RESULTS AND DISCUSSIONS

414 In this study, a total of 16,766 neuroimaging (MRI) data consisting of three classes (AD, MCI,
415 and CN) were used. Three different CNN models were tested for use in the early diagnosis of AD.
416 Using Python 3.7, the scikit-learn library, and TensorFlow, the models were trained within the
417 Google Colab framework. This platform offers quantitative tools and adaptable resource allocation
418 to manage usage limits and hardware accessibility. In addition, several Python libraries, including
419 Pandas, NumPy, Matplotlib, and Keras, were used to build deep learning models. To work with

420 NIFTI image files, images with the .nii extension were converted to PNG. PNG images were
421 resized to 224×224 . Images converted to PNG in the dataset were matched to class labels in the
422 CSV file. After the labeling processes were completed, the three selected models were run. Some
423 MRI images of AD, MCI, and CN cases in the dataset are provided in Fig. 2.

424 Figure 2. Examples of AD, MCI, and CN MRI images.

425 A general architecture of the CNN model is presented in Fig. 3.

426 Figure 3. CNN architecture.

427 The selected models (EfficientNetB0, DenseNet121, AlexNet) were run for 50 epochs, and the
428 detailed status of the training and test results obtained are given in Tables 3 and 4.

429 Table 3. Training results when models run.

430 Table 4. Testing results when models run.

431 When the training and test results were examined, we found that the AlexNet model had the
432 highest accuracy value during the training. After examining the accuracy values of the test results,
433 we found that the DenseNet121 model performed well. The DenseNet121 model achieved a high
434 MCC value of 0.97. MCC takes a value between 0 and 1 when measuring the performance of a
435 classification model (Chicco & Jurman, 2020); the closer the MCC value is to 1, the better the
436 model's classification performance. In the case of DenseNet121, an MCC value of 0.97 indicated
437 that the model had a notably high classification performance, the model's predictions were highly
438 correlated with true classes, and there was a strong correlation between true positives and true
439 negatives. It also highlighted the classification accuracy and reliability of the model. Table 4 shows
440 that the precision value for the DenseNet121 model is 98.19%. The higher the precision value, the
441 lower the probability of false-positive prediction in the model. A higher recall indicates fewer false
442 negative predictions and more true negative predictions. The F1 score is high when both precision
443 and recall are high. When these values are analyzed, the results are promising. The AUC value
444 was computed as 98.22% for the DenseNet121 model; an AUC value close to 1 led us to conclude
445 that the results were good (Ling et al. 2003).

446 Confusion matrices obtained for all models are given in Fig. 4.

447 Figure 4. (A) EfficientNetB0 model, (B) DenseNet121 model, and (C) AlexNet model.

448 According to the confusion matrices in Fig. 4, the DenseNet121 model correctly classified 1705
449 of 1716 AD images, 1576 of 1609 MCI images, and 1658 of 1705 CN images. In the study by
450 Savaş et al. (2022), 92.98% accuracy was obtained with the EfficientNetB0 model, and 91.91%
451 accuracy was obtained with the EfficientNetB1 model for CN, MCI, and AD classification. In our
452 study, an accuracy of 97.33% was obtained with the EfficientNetB0 model. In the study by Khan
453 et al. (2022), 95.75% accuracy was obtained with a hybrid model for CN, MCI, and AD
454 classification, whereas the highest accuracy rate was 98.19% with the DenseNet121 model in our
455 study. Thus, our study achieved better results than both previous studies.

456 After the images were processed through the models, the models were run using one-versus-one
457 classification, in which each class was compared with another class. Table 5 shows the results of

458 the one-versus-one classification obtained from the training. Table 6 shows the results of the one-
459 versus-one classification obtained from the testing.

460 Table 5. Training results obtained from running models for one-versus-one classification.

461 Table 6. Testing results obtained from running models for one-versus-one classification.

462 The results demonstrated that the EfficientNetB0 model provided satisfactory results in three
463 classifications and high accuracy values for CN vs. AD and MCI vs. AD classification. The
464 DenseNet121 model also provided a high accuracy rate of 98.42% for CN vs. MCI classification.
465 Table 6 shows that the precision value for the EfficientNetB0 model in CN-AD classification is
466 98.94%, and the AUC value is 98.90%. The table also shows the precision value for the
467 EfficientNetB0 model in the MCI-AD classification, which is 97.95%; the AUC value is 98.00%.
468 In CN-MCI classification, the precision value for the DenseNet121 model is 98.42%, and the AUC
469 value is 98.40%. The higher the precision value, the lower the probability that the model will
470 predict false positives. A higher recall indicates fewer false negative predictions and more true
471 negative predictions. The F1 score is high when both precision and recall are high. According to
472 these values in our results, it can be concluded that satisfactory results were obtained.

473 Confusion matrices obtained when the models were classified as one-versus-one are given in
474 Figs. 5–7.

475 Figure 5. One-versus-one classification confusion matrices (CN-AD) for the (A) EfficientNetB0, (B)
476 DenseNet121, and (C) AlexNet models.

477 According to the confusion matrices in Figure-5, 1716 AD to 1689 AD were classified correctly
478 using the EfficientNetB0 model. The DenseNet121 model classified 1680 of 1716 AD patients
479 correctly. The lowest validation rate in AD vs. CN classification was obtained with the
480 DenseNet121 model.

481 Figure 6. One-versus-one classification confusion matrices (MCI-AD) for the (A) EfficientNetB0, (B)
482 DenseNet121, and (C) AlexNet models.

483 In the classification of AD vs. MCI, the EfficientNetB0 model had the best classification results,
484 and the DenseNet121 model had the worst classification results. The complexity matrix of the
485 DenseNet121 model in Figure 6 shows that 1575 of 1716 AD patients were classified correctly.

486 Figure 7. One-versus-one classification confusion matrices (CN-MCI) for the (A) EfficientNetB0, (B)
487 DenseNet121, and (C) AlexNet models.

488 The most accurate classification of CN vs. MCI was provided by the DenseNet121 model,
489 according to Fig. 7B. In the complexity matrix of the DenseNet121 model, it is shown that 1577
490 of 1606 MCI classes were correctly classified. The most inaccurate classification was obtained
491 with the AlexNet model.

492 After the models were run using the one-versus-one classification, they were run using one-
493 versus-all classification. In the one-versus-all classification, each class formed a group, and all the
494 remaining classes were combined. Table 7 shows the results of the one-versus-all classification

495 obtained from the training. Table 8 shows the results of the one-versus-all classification obtained
496 from the testing.

497 Table 7. Training results obtained from running models for one-versus-all classification.

498 Table 8. Testing results obtained from running models for one-versus-all classification.

499 The DenseNet121 model for testing achieved excellent accuracy in both MCI vs. CN-AD and
500 CN vs. MCI-AD one-versus-all classifications. Table 8 shows that the precision value achieved
501 with the DenseNet121 model for MCI-CNAD classification was 98.40%, and the AUC value for
502 this model was 98.00%. Table 8 shows that the precision value of the AlexNet model for AD-CN-
503 MCI classification was 99.58%, and the AUC value was 99.50%. For CN-MCI-AD classification,
504 the precision and AUC values for the DenseNet121 model were 97.83%, and 96.80%, respectively.

505 The confusion matrices obtained when the models were classified as one-versus-all are given in
506 Figs. 8–10.

507 Figure 8. One-versus-all classification confusion matrices (MCI-CN-AD) for the (A) EfficientNetB0, (B)
508 DenseNet121, and (C) AlexNet models.

509 Figure 8 shows that the DenseNet121 model achieved the best MCI vs. CN-AD classification
510 performance. With the DenseNet121 model, out of 1609 CN-AD classes, 1556 were correctly
511 classified, and for the MCI class, 3394 of 3421 classes were classified correctly. On the other hand,
512 the worst classification performance was obtained using the AlexNet model. The AlexNet model
513 correctly classified 1035 of 1609 CN-AD classes, and for the MCI class, 3405 of 3421 classes
514 were classified correctly.

515 Figure 9. One-versus-all classification confusion matrices (AD-CN-MCI) for the (A) EfficientNetB0, (B)
516 DenseNet121, and (C) AlexNet models.

517 Figure 9 shows that the AlexNet model achieved the best classification performance in the AD
518 vs. CN-MCI classification. For the AlexNet model, of 1716 CN-MCI classes, 1705 were correctly
519 classified, and 3304 of 3314 classes were classified correctly for the AD class. On the other hand,
520 the worst classification performance was obtained using the EfficientNetB0 model. For the
521 EfficientNetB0 model, 1688 of 1716 CN-MCI classes were correctly classified, and for the AD
522 class, 3282 of 3314 classes were classified correctly.

523 Figure 10. One-versus-all classification confusion matrices (CN-MCI-AD) for the (A) EfficientNetB0,
524 (B) DenseNet121, and (C) AlexNet models.

525 Figure 10 shows that the DenseNet121 model achieved the best classification performance for
526 CN vs. MCI-AD classification. For this model, of 3325 MCI-AD classes, 3322 were correctly
527 classified, and 1599 of 1705 classes were classified correctly for the CN class. On the other hand,
528 the worst classification performance was obtained using the AlexNet model. For this model, in CN
529 vs. MCI-AD classification, 3318 of 3325 MCI-AD classes were correctly classified, and for the
530 CN class, only 1538 of 1705 classes were classified correctly.

531 When using one-versus-one classification, the EfficientNetB0 model provided the best results,
532 with 98.94% accuracy for CN vs. AD classification. The EfficientNetB0 model also provided the

533 best results for MCI vs. AD classification, with 97.95% accuracy. Finally, the DenseNet121 model
 534 provided the best results for CN vs. MCI classification, with 98.42% accuracy. Through analyzing
 535 these results, we determined that these high accuracy values are different because each
 536 classification task has different dynamics, and the data distribution of each class is different. AD
 537 vs. MCI classification accuracy is lower than the others because the distinction between an
 538 individual with AD and an individual with a mild stage of this disease is more complex.

539 In this study, McNemar's Test was used as the nonparametric statistical variant of the χ^2 test to
 540 determine the statistical significance between the performances of the classifiers. When comparing
 541 the performances of two classifiers, four possible outputs exist. These outputs can be seen in Table
 542 9.

543 Table 9. Possible outcomes of two classifiers.

544 As shown in Table 9, N_{ff} , N_{sf} , N_{fs} , and N_{ss} represent the number of times both classifiers failed
 545 to predict, only classifier A succeeded, only classifier B succeeded, and both classifiers succeeded,
 546 respectively. However, only N_{sf} and N_{fs} values were used to obtain a significant difference because
 547 these values represented the number of times a classifier succeeded and another failed. N_{sf} and N_{fs}
 548 values were employed to calculate the z-score, which represents whether two classifiers show
 549 similar performance, as shown in Equation (6):

$$550 \quad Z = \frac{(|N_{sf} - N_{fs}| - 1)}{\sqrt{N_{sf} + N_{fs}}} \quad (6)$$

551 If the z-score equals 0, this situation is accepted because the two classifiers show similar
 552 performance. As the z-score diverges from 0, the performance difference of the two classifiers
 553 becomes more significant. In addition, z-scores can be interpreted according to the confidence
 554 levels for one-tailed and two-tailed predictions. In Table 10, confidence levels corresponding to
 555 the z-scores are presented.

556 Table 10. Z-scores and confidence levels.

557 The z-scores of the architectures for AD prediction are given in Tables 11 and 12.

558 Table 11. Z-scores of architectures for AD prediction for one-versus-one classification.

559 Table 12. Z-scores of architectures for AD prediction for one-versus-all classification.

560 Tables 11 and 12 compare the performance of different classifiers on the given dataset, using
 561 arrowheads (\leftarrow , \uparrow) to indicate which classifier performed better in terms of true predictions (both
 562 true positives and true negatives). The z-scores next to the arrowheads measure how statistically
 563 significant the results are. Furthermore, statistically significant results are written in bold in the
 564 tables. If the results are statistically significant, the confidence levels are included below for both
 565 one-tailed and two-tailed predictions.

566 Table 11 represents the one-versus-one classification results of the three deep learning
 567 architectures for CN vs. AD, CN vs. MCI, and MCI vs. AD classification. The results of CN vs.
 568 AD classification shown in Table 11 demonstrate that EfficientNetB0 performed better than

569 DenseNet121 and AlexNet. In addition, the performance differences between EfficientNetB0 and
570 the other architectures were statistically significant for CN and AD classification. Z-score values
571 of 5.86 and 4.44 indicate 99.5% and 99% confidence levels. AlexNet demonstrated higher
572 performance than DenseNet121, and this performance difference is statistically significant, with
573 confidence levels of 95% and 90%.

574 When we analyzed the results of CN vs. MCI, as shown in Table 11, we concluded that
575 DenseNet121 performed better than both EfficientNetB0 and AlexNet. In addition, the
576 performance differences between DenseNet121 and the other architectures were statistically
577 significant for CN and MCI classification. Z-score values of 3.66 and 5.23 indicate 99.5% and
578 99% confidence levels. EfficientNetB0 demonstrated higher performance than AlexNet, and this
579 performance difference is statistically significant, with confidence levels of 95% and 90%.

580 After examining the results of MCI vs. AD classification, as shown in Table 11, we concluded
581 that EfficientNetB0 performed better than both DenseNet121 and AlexNet. However, the
582 performance difference between EfficientNetB0 and AlexNet was statistically significant with a
583 z-score of 1.31. In contrast, the performance difference between EfficientNetB0 and DenseNet121
584 was statistically significant, with confidence levels of 99.5% and 99% for MCI and AD
585 classification. AlexNet demonstrated higher performance than DenseNet121, and this performance
586 difference is statistically significant, with confidence levels of 99.5% and 99%.

587 Table 12 represents the one-versus-all classification results of the three deep learning
588 architectures for CN vs. all, MCI vs. all, and AD vs. all.

589 As shown in Table 12, the results of CN vs. MCI-AD classification demonstrate that
590 DenseNet121 outperformed the other architectures. The performance difference between
591 DenseNet121 and EfficientNetB0 was not found to be statistically significant, with a z-score of
592 0.86, whereas the performance difference between DenseNet121 and AlexNet was found to be
593 statistically significant, with confidence levels of 99.5% and 99% for CN and other (MCI-AD)
594 classification. Furthermore, EfficientNetB0 outperformed AlexNet, and the performance
595 difference was statistically significant, with confidence levels of 99.5% and 99%.

596 The results of MCI vs. CN-AD classification, as shown in Table 12, demonstrate that
597 DenseNet121 outperformed the other architectures. The performance differences between
598 DenseNet121 and the other architectures were statistically significant, with confidence levels of
599 99.5% and 99% for MCI and other (CN-AD) classifications. Furthermore, EfficientNetB0
600 outperformed AlexNet, and the performance difference was found to be statistically significant,
601 with confidence levels of 99.5% and 99%.

602 In addition, the results shown in Table 12 demonstrate that AlexNet outperformed the other
603 architectures in AD vs. CNMCI classification. The performance difference between AlexNet and
604 DenseNet121 was not statistically significant, with a z-score of 0.70 for AD and other (CN-MCI)
605 classifications. However, the performance difference between AlexNet and EfficientNetB0 was
606 found to be statistically significant, with confidence levels of 99.5% and 99%. Furthermore,
607 DenseNet121 outperformed EfficientNetB0, and the performance difference was statistically
608 significant, with confidence levels of 99.5% and 99%.

609 Mora-Rubio et al. (2023) obtained an accuracy of 89.02% with the vision transformer (ViT) in
610 AD classification vs. CN. In our study, the EfficientNetB0 model achieved an accuracy of 98.94%
611 for CN vs. AD classification. At the same time, Mora-Rubio et al. (2023) obtained an accuracy of
612 66.41% with DenseNet and EfficientNet models for MCI vs. CN classification. Our result was an
613 accuracy of 98.42% obtained with the DenseNet121 model for MCI vs. CN classification. We
614 obtained better results in one-versus-one classification, which may be due to the differences in the
615 numbers in the dataset, model architectures used, and testing and training processes. When our
616 results are compared with other studies in the literature (Savaş, 2022), the highest average accuracy
617 rate of 92.98% was achieved using the EfficientNetB0 model, whereas Khan et al. (2022) reported
618 a maximum average accuracy rate of 95.75%, which was obtained using an XGB + DT + SVM
619 hybrid model.

620 Compared with these results, our average accuracy rate with the DenseNet121 model was
621 98.19%. The EfficientNetB0 model follows, with an average accuracy rate of 97.33%. Our results
622 show better performance compared with those of previous studies. Our choice of preferred models
623 compared with the models used in the study by Khan et al. (2022) allowed us to obtain better
624 results. At the same time, the selection of more recent models might have also affected our results.
625 When examining the results of other studies, it can be observed that in the work of Mehmood et
626 al. (2021), a 98.73% accuracy rate was achieved for the classification of CN vs. AD. In addition,
627 Sethi et al. (2022) reported an accuracy rate of 89.40% for AD vs. CN classification.

628 Furthermore, Naz et al. (2021) obtained an accuracy of 98.89% using the VGG-16 model and
629 91.38% using the AlexNet model in AD vs. CN classification. These findings indicate that our
630 study produced better results in the classification of AD vs. CN compared with the results reported
631 in the literature. In addition, the EfficientNetB0 model achieved a better result in CN vs. AD
632 classification, with an accuracy rate of 98.94%.

633 Regarding MCI vs. AD classification, Naz et al. (2021) obtained a slightly higher accuracy result
634 of 99.27% using the VGG-19 model. They obtained an accuracy of 97.06% in the classification of
635 CN vs. MCI; in our study, an accuracy of 98.42% was obtained with the EfficientNet121 model.
636 Because it is important to distinguish between a CN subject and a subject with MCI, the high
637 classification accuracy of CN vs. MCI marks an important contribution. In addition, studies in the
638 literature using one-versus-all classification are limited for the related problem. Promising results
639 have been obtained for this type of classification in our study.

640 In the study by Islam & Zhang (2017), the OASIS dataset was used. They performed the
641 classification with a total of four classes and 416 subjects. By proposing their model framework,
642 the best result of 73.75% was achieved in 10 epochs using 5-fold cross-validation. In our study,
643 there were three classes in total conducted on the ADNI dataset. After necessary operations were
644 performed on the 16,766 MRI images in the dataset, the three models were run by separating the
645 dataset into 70% for training and 30% for testing. When examining the results, our approach
646 outperformed that of the study by Islam & Zhang (2017). More MRI images were used in our study
647 than in theirs. Larger datasets have the potential to reduce a model's tendency to memorize; when

648 a model is trained with more data, it tends to learn general patterns and features rather than
649 memorizing situations during the learning process.

650 In a study conducted by Mamun et al. (2022), 6219 MRI images with four classes were used.
651 The dataset was first preprocessed by performing image resizing, noise removal, image
652 segmentation, and smoothing. They trained the dataset using the holdout cross-validation method
653 and obtained results using a CNN architecture. The highest accuracy of 97.60% was achieved with
654 their approach. In our study, a general average accuracy rate of 98.19% was obtained using the
655 DenseNet121 model. The one-versus-one and one-versus-all classification accuracies were higher
656 than the results obtained in this study. Another difference between our study and the study by
657 Mamun et al. (2022) is that we used more MRI images with three classes, and the dataset was
658 divided into 70% for training and 30% for testing when running the models. In addition, the
659 EfficientNetB0, DenseNet121, and AlexNet models were employed to perform the one-versus-
660 one and one-versus-all classifications.

661 Sekhar & Jagadev (2023) used a dataset of 6400 MRI images for the classification of AD by
662 dividing the dataset into training, testing, and validation portions. They proposed their own neural
663 network. They also stated that the advantage of end-to-end learning is that it can create an effective
664 visual explanation of the logic behind the classification results obtained by CNN, which will help
665 doctors understand the impact of CNN and find new biomarkers. The best result of 98.5% was
666 obtained with the EfficientNet model. In our study, an accuracy of 98.94% was achieved with the
667 EfficientNetB0 model in CN-AD classification for one-versus-one classification. Furthermore, an
668 accuracy of 99.58% was obtained using the AlexNet model in AD-CN-MCI one-versus-all
669 classification. This shows that considerable improvements have been made in our study compared
670 with the results of others in the literature.

671 The results of our study clearly demonstrate that the DenseNet121 model provides the worst
672 results for one-versus-one classification (MCI vs. AD), with an accuracy of 90.75%. AD diagnosed
673 at an early stage can improve patients' quality of life and slow the progression of the disease. Our
674 study obtained the best CN vs. MCI and CN vs. AD classification results. Because it is important
675 to distinguish between CN and MCI, the accuracy rate obtained in this study is a significant
676 contribution to the literature. Early detection of the disease in the mild stage is also an important
677 tool for preventing the progression of AD. When it comes to distinguishing between a patient with
678 AD and a patient with MCI, determining which class they belong to becomes more challenging.
679 In contrast, for less complex cases, better results were achieved, and the classification process was
680 relatively easier.

681 **CONCLUSION AND FUTURE WORK**

682 This study aims to enable early detection and classification of AD using CNN-based methods.
683 The ADNI-3 dataset was utilized, which consisted of T1-weighted structural MRI data and axial
684 brain slices from 515 individuals.

685 Within the scope of this study, the images in NIFTI format within the dataset were converted to
686 PNG format as the preliminary step. Each converted image was resized to a dimension of $224 \times$

687 224. The PNG images were paired with their corresponding class labels in the CSV file. The
688 dataset was split into 70% for training and 30% for testing, and results were obtained with the
689 models determined in the next stages. Results were obtained from the models using both one-
690 versus-one classification and one-versus-all classification.

691 Satisfactory results were obtained for CN vs. MCI one-versus-one classification. A significant
692 finding was the ability to distinguish a healthy person from someone with MCI. Early detection of
693 AD, before progression in MCI individuals, is a major contribution of this study. A one-versus-
694 one classification can be an important tool in early diagnosis, management, treatment, and research
695 on AD. Such classifications can potentially reduce the disease's effects and improve patients'
696 quality of life. In addition, some important factors must be considered before the models are
697 clinically applicable. One of these is that the model should provide a high accuracy rate and
698 produce reliable results. In some clinical settings, misleading results, erroneous diagnoses, and
699 predictions are unacceptable. Likewise, in some clinical applications, medical experts can analyze
700 MRI images to determine the AD status of patients. By examining the results of the model, medical
701 experts can see possible signs of AD and then support their diagnosis by initiating the necessary
702 medical procedures. The results of the model can be combined with the medical experts' clinical
703 experience and patient history and then used to assist in making the final diagnosis. Therefore, we
704 believe that these models can be of significant benefit in the clinical setting.

705 McNemar's test is an important tool for comparing and evaluating the accuracy of classification
706 models. A nonparametric statistical variant of the χ^2 test, McNemar's test, was used to determine
707 the statistical significance between the performances of the classifiers. McNemar's test is useful
708 at this point because it is important to evaluate whether the difference between the models is
709 statistically significant, enabling researchers to choose the right model and make decisions for
710 development. The overall results obtained for the early detection of AD are promising, and it is
711 anticipated that they could be adapted to a more general approach with different test datasets.
712 Although the model's results are satisfactory, expanding the dataset might lead to even better
713 outcomes.

714 In future research, we plan to focus on augmenting the dataset using generative adversarial
715 networks (GAN) to generate artificial MRI images. The potential benefits of using GAN-generated
716 images in the study will be investigated.

717

718

719

720 **ADDITIONAL INFORMATION AND DECLARATIONS**

721

722 **Funding**

723 The authors received no funding for this work.

724

725 **Competing Interests**

726 The authors declare that they have no competing interests.

727

728 Data Availability

729 The following information on data availability was provided: The data is available from ADNI
730 (<https://adni.loni.usc.edu>).

731 Github access to the dataset: [https://github.com/Begumer/Alzheimer-s-Disease-](https://github.com/Begumer/Alzheimer-s-Disease-Classification/tree/main)
732 [Classification/tree/main](https://github.com/Begumer/Alzheimer-s-Disease-Classification/tree/main)

733 The search parameters for ADNI database are available at Zenodo: Begüm Şener. (2023). First
734 Release (v1.0). Zenodo. <http://doi.org/10.5281/zenodo.10259112>

735

736 REFERENCES

737

738 Albawi, S., Mohammed, T. A., Al-Zawi, S. 2017. Understanding of a convolutional neural
739 network. *2017 International Conference on Engineering and Technology (ICET)* [Preprint].
740 doi:10.1109/icengtechnol.2017.8308186.

741

742 Basha, S. H. S., Dubey, S. R., Pulabajgari, V., Mukherjee, S. 2020. Impact of fully connected
743 layers on performance of convolutional neural networks for Image Classification.
744 *Neurocomputing*, 378, pp. 112–119. doi:10.1016/j.neucom.2019.10.008.

745

746 Bostanci, B., Bostanci, E. 2012. An evaluation of classification algorithms using MC Nemar's test.
747 *Advances in Intelligent Systems and Computing*, pp. 15–26. doi:10.1007/978-81-322-1038-2_2.

748

749 Buxton, R. B., Edelman, R. R., Rosen, B. R., Wismer, G.L. Brady, T. J. 1987. Contrast in
750 rapid MR imaging: T1-and T2-weighted imaging. *Journal of Computer Assisted Tomography*,
751 11(1), pp. 7–16. doi:10.1097/00004728-198701000-00003.

752

753 Chicco, D., & Jurman, G. 2020. The advantages of the Matthews correlation coefficient (MCC)
754 over
755 F1 score and accuracy in binary classification evaluation. *BMC genomics*, 21(1), 1-13. doi:
756 10.1186/s12864-019-6413-7.

757

758 Colligris, P., Perez de Lara, M. J., Colligris, B., Pintor, J. 2018. Ocular manifestations of
759 alzheimer's and other neurodegenerative diseases: The prospect of the eye as a tool for the early
760 diagnosis of alzheimer's disease. *Journal of Ophthalmology*, 2018, pp. 1–12.
761 doi:10.1155/2018/8538573.

762

763 Costa, C. D. Best Python libraries for machine learning and deep learning. Online Access:
764 [https://towardsdatascience.com/best-python-libraries-for-machine-learning-and-deep-learning-](https://towardsdatascience.com/best-python-libraries-for-machine-learning-and-deep-learning-b0bd40c7e8c)
765 [b0bd40c7e8c](https://towardsdatascience.com/best-python-libraries-for-machine-learning-and-deep-learning-b0bd40c7e8c) (Date of Access: February 2023).

766

767 Cummings, J. L., & Cole, G. 2002. Alzheimer disease. *JAMA*, 287(18), p. 2335.
768 doi:10.1001/jama.287.18.2335.

769

- 770 Farooq, A., Anwar, S., Awais, M., Rehman, S. 2017. A deep CNN based multi-class classification
771 of alzheimer's disease using MRI. *2017 IEEE International Conference on Imaging Systems and*
772 *Techniques (IST)* [Preprint]. doi:10.1109/ist.2017.8261460.
773
- 774 Hart, D. J., Craig, D., Compton, S. A., Critchlow, S., Kerrigan, B. M., Mcllroy, S. P., Passmore,
775 A. P. 2003. A retrospective study of the behavioural and psychological symptoms of mid and
776 late phase alzheimer's disease. *International Journal of Geriatric Psychiatry*, 18(11), pp. 1037
777 1042. doi:10.1002/gps.1013.
778
- 779 Islam, J., & Zhang, Y. 2017. A novel deep learning based multi-class classification method for
780 Alzheimer's disease detection using brain MRI data. In *Brain Informatics: International*
781 *Conference, BI*
782 *2017, Beijing, China, November 16-18, Proceedings* (pp. 213-222). Springer International
783 Publishing. doi:10.1007/987-3-319-70772-3_20.
784
- 785 Khan, Y. F., Kaushik, B., Chowdhary, C. L., Srivastava, G. 2022. Ensemble model for diagnostic
786 classification of alzheimer's disease based on brain anatomical magnetic resonance imaging
787 *Diagnostics*, 12(12), p. 3193. doi:10.3390/diagnostics12123193.
788
- 789 Li, F., Cheng, D., Liu, M. 2017. Alzheimer's disease classification based on combination of multi-
790 model convolutional networks. *2017 IEEE International Conference on Imaging Systems and*
791 *Techniques (IST)* [Preprint]. doi:10.1109/ist.2017.8261566.
792
- 793 Ling, C. X., Huang, J., Zhang, H. 2003. AUC: a statistically consistent and more discriminating
794 measure than accuracy. In *Ijcai* (Vol. 3, pp. 519-524).
795
- 796 Lingras, P., Butz, C. 2007. Rough set based 1-V-1 and 1-V-R approaches to support vector
797 machine multi-classification. *Information Sciences*, 177(18), pp. 3782-3798.
798 doi:10.1016/j.ins.2007.03.028.
- 799 Maharjan, S., Alsadoon, A., Prasad, P. W. C., Al-Dalain, T., Alsadoon, O. H. 2020. A novel
800 enhanced softmax loss function for brain tumour detection using Deep Learning. *Journal of*
801 *Neuroscience Methods*, 330, p. 108520. doi:10.1016/j.jneumeth.2019.108520.
802
- 803 Mamun, M., Shawkat, S. B., Ahammed, M. S., Uddin, M. M., Mahmud, M. I., Islam, A. M. 2022.
804 Deep Learning Based Model for Alzheimer's Disease Detection Using Brain MRI Images. In *2022*
805 *IEEE 13th Annual Ubiquitous Computing, Electronics & Mobile Communication Conference*
806 *(UEMCON)* (pp. 0510-0516). doi:10.1109/UEMCON54665.2022.9965730.
807
- 808 Marques, G., Agarwal, D., De la Torre Díez, I. 2020. Automated medical diagnosis of COVID-19
809 through EfficientNet Convolutional Neural Network. *Applied Soft Computing*, 96, p. 106691.
810 doi:10.1016/j.asoc.2020.106691.
- 811 Mehmood, A., Yang, S., Feng, Z., Wang, M., Ahmad, A. S., Khan, R., Yagub, M. 2021. A
812 transfer learning approach for early diagnosis of alzheimer's disease on MRI images.
813 *Neuroscience*, 460, pp. 43-52. doi:10.1016/j.neuroscience.2021.01.002.
814
- 815 Mohammadjafari, S., Cevik, M., Thanabalasingam, M., Basar, A. 2021. Using ProtoPNet for

- 816 interpretable alzheimer's disease classification. *Proceedings of the Canadian Conference on*
817 *Artificial Intelligence* [Preprint]. doi:10.21428/594757db.fb59ce6c.
818
- 819 Mohi ud din dar, G., Bhagat, A., Ansarullah, S. I., Othman, M. T. B., Hamid, Y., Alkahtani, H. K.,
820 Hamam, H. 2023. A novel framework for classification of different alzheimer's disease stages
821 using CNN model. *Electronics*, 12(2), p. 469. doi:10.3390/electronics12020469.
822
- 823 Mora-Rubio, A., Bravo-Ortíz, M. A., Arredondo, S. Q., Torres, J. M. S., Ruz, G. A., Tabares-Soto,
824 R. 2023. Classification of Alzheimer's disease stages from magnetic resonance images using deep
825 learning. *PeerJ Computer Science*, 9, e1490.
826
- 827 Naz, S., Ashraf, A., Zaib, A. 2021. Transfer learning using freeze features for alzheimer
828 neurological disorder detection using ADNI dataset. *Multimedia Systems*, 28(1), pp. 85–94.
829 doi:10.1007/s00530-021-00797-3.
830
- 831 Omonigho, E. L., David, M., Adejo, A., Saliyu, A. 2020. Breast cancer:tumor detection in
832 mammogram images using modified Alexnet Deep Convolution Neural Network. *2020*
833 *International Conference in Mathematics, Computer Engineering and Computer Science*
834 *(ICMCECS)* [Preprint]. doi:10.1109/icmcecs47690.2020.240870.
835
- 836 Savaş, S. 2022. Detecting the stages of alzheimer's disease with pre-trained Deep Learning
837 Architectures. *Arabian Journal for Science and Engineering*, 47(2), pp. 2201–2218.
838 doi:10.1007/s13369-021-06131-3.
839
- 840 Sethi, M., Rani, S., Singh, A., Mazon, J. L. V. 2022. A CAD system for alzheimer's disease
841 classification using neuroimaging MRI 2D slices. *Computational and Mathematical Methods in*
842 *Medicine*, 2022, pp. 1–11. doi:10.1155/2022/8680737.
843
- 844 Sekhar, B. V. D. S., Jagadev, A. K. 2023. Efficient Alzheimer's disease detection using deep
845 learning technique. *Soft Computing*, 1-8. doi:10.1007/s00500-023-08434-z.
846
- 847 Shanmugam, J. V., Duraisamy, B., Simon, B. C., Bhaskaran, P. 2022. Alzheimer's disease
848 classification using pre-trained Deep Networks. *Biomedical Signal Processing and Control*, 71,
849 p. 103217. doi:10.1016/j.bspc.2021.103217.
850
- 851 Solano-Rojas, B., Villalón-Fonseca, R., Marín-Raventós, G. 2020 Alzheimer's disease early
852 detection using a low cost three-dimensional Densenet-121 architecture. *Lecture Notes in*
853 *Computer Science*, pp. 3–15. doi:10.1007/978-3-030-51517-1_1.
854
- 855 Sun, M., Song, Z., Jiang, X., Pan, J., Pang, Y. 2017. Learning pooling for Convolutional Neural
856 Network. *Neurocomputing*, 224, pp. 96–104. doi:10.1016/j.neucom.2016.10.049.
857 TensorFlow. Available online: <https://www.tensorflow.org/?hl=ar> (Date of Access: February
858 2023).

Figure 1

Research Methodology

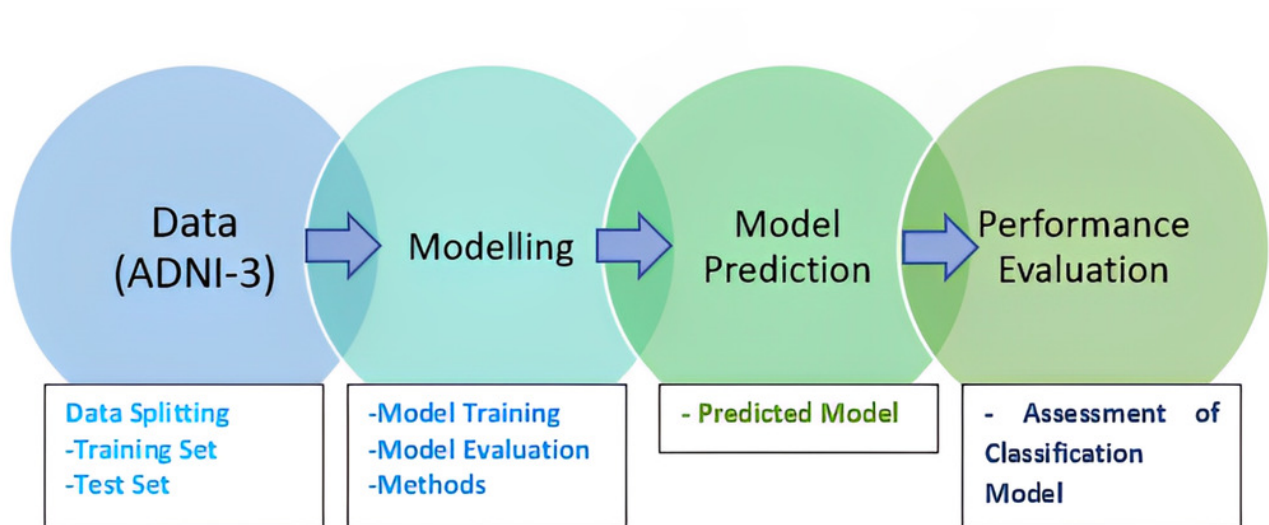


Figure 2

Examples of AD, MCI, and CN MRI images

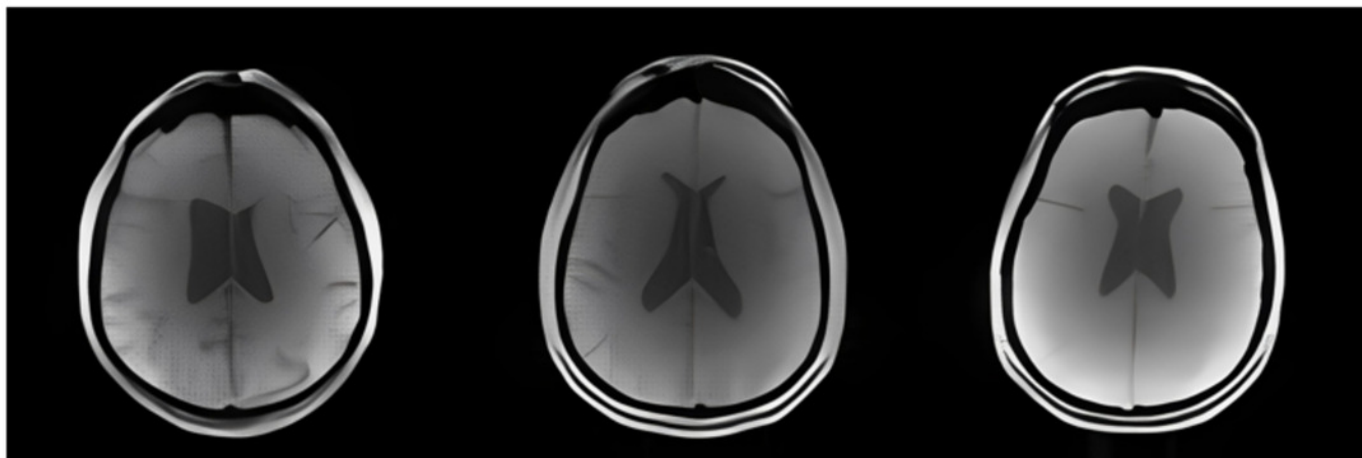


Figure 3

CNN Architecture

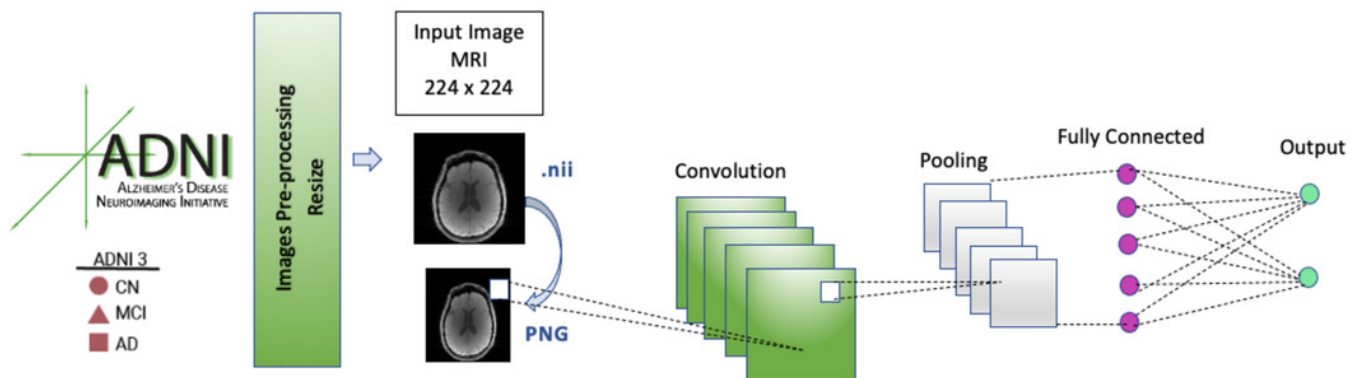


Figure 4

Confusion matrices

(A) EfficientNetB0 model (B) DenseNet121 Model (C) AlexNet Model

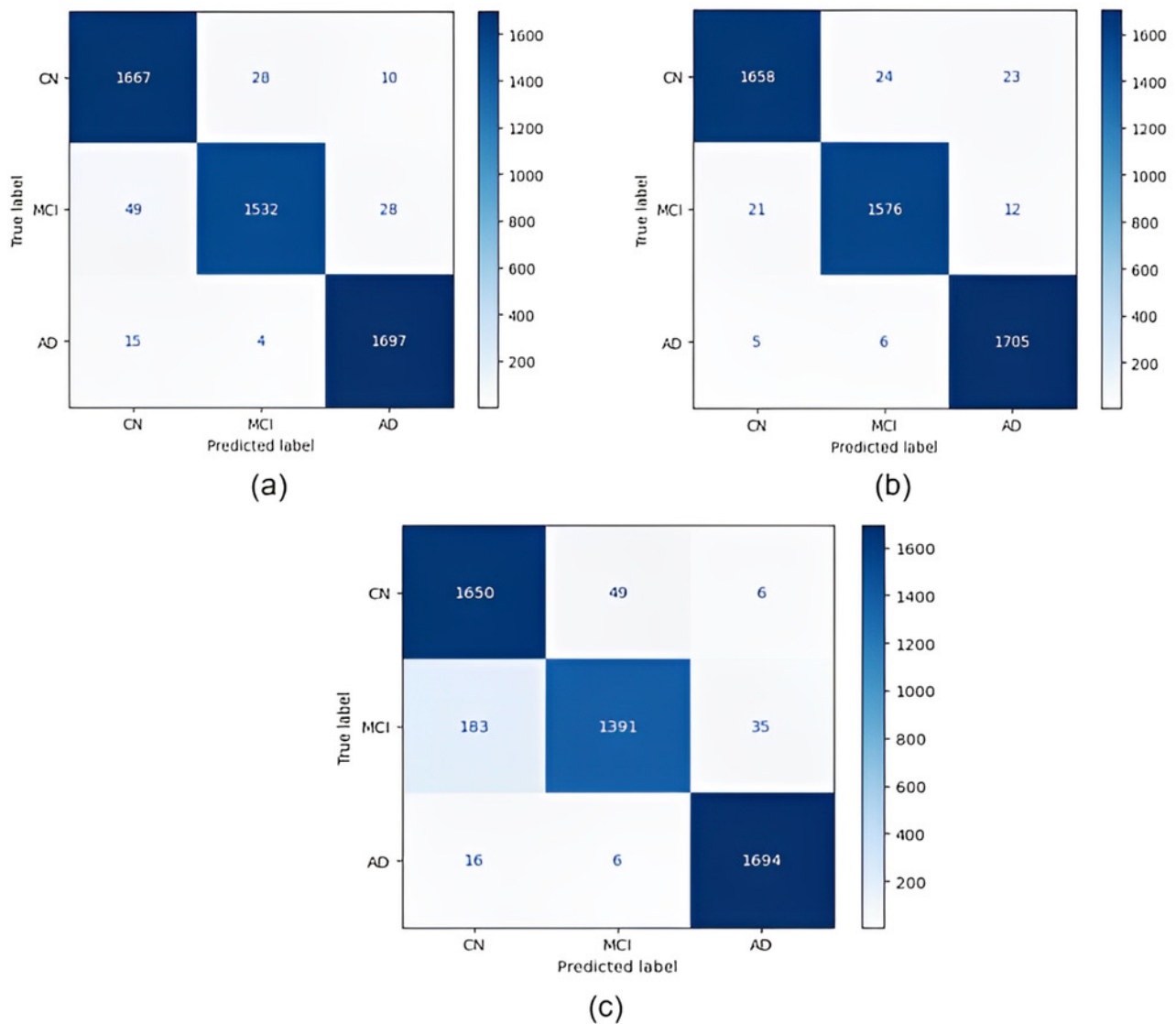


Figure 5

1 vs 1 classification confusion matrices (CN/AD)

1 vs 1 classification confusion matrices (CN/AD) for (A) EfficientNetB0 model (B) DenseNet121 model (C) AlexNet model

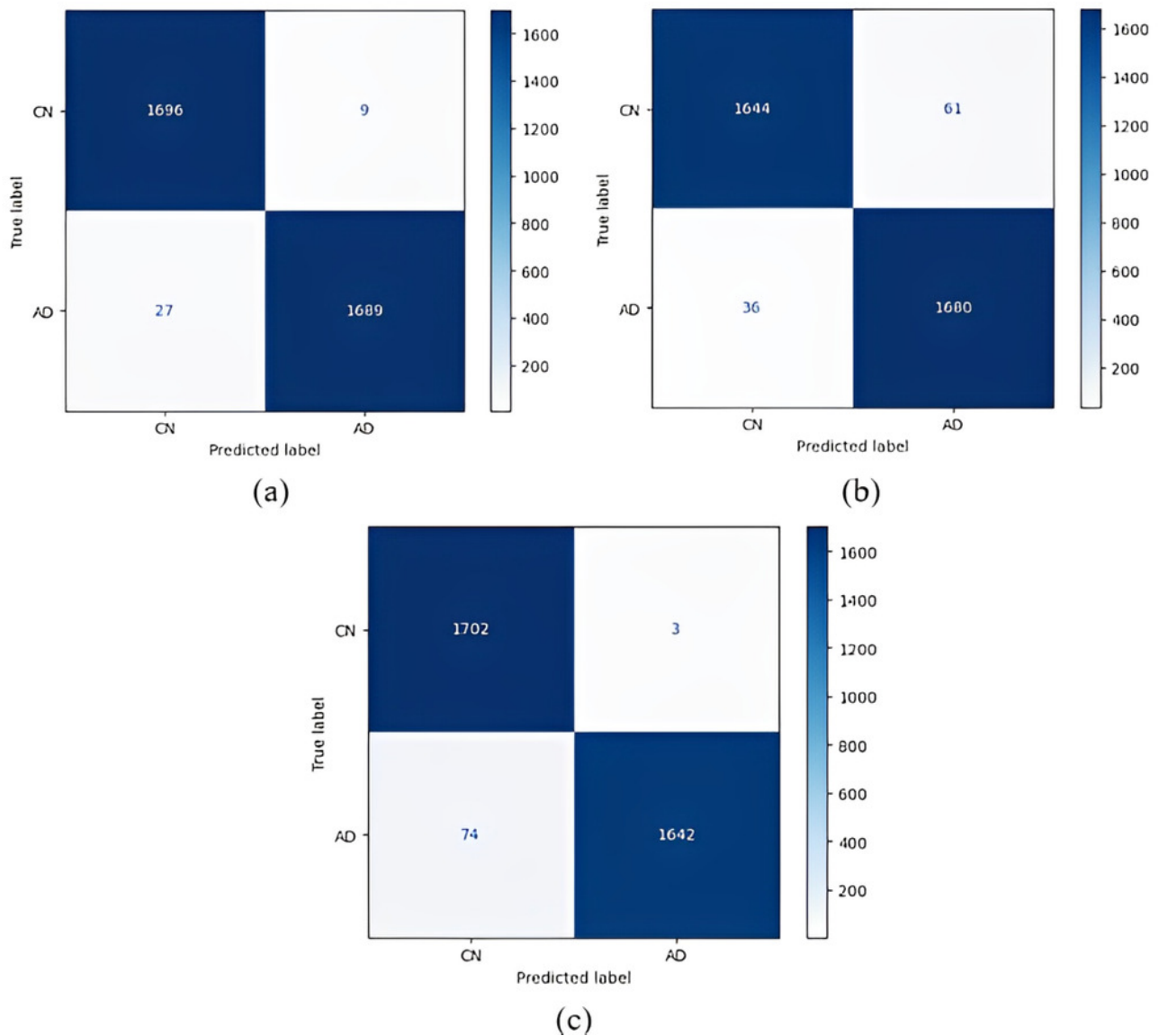


Figure 6

1 vs 1 classification confusion matrices (MCI/AD)

1 vs 1 classification confusion matrices (MCI/AD) for (A) EfficientNetB0 model (B) DenseNet121 model (C) AlexNet model

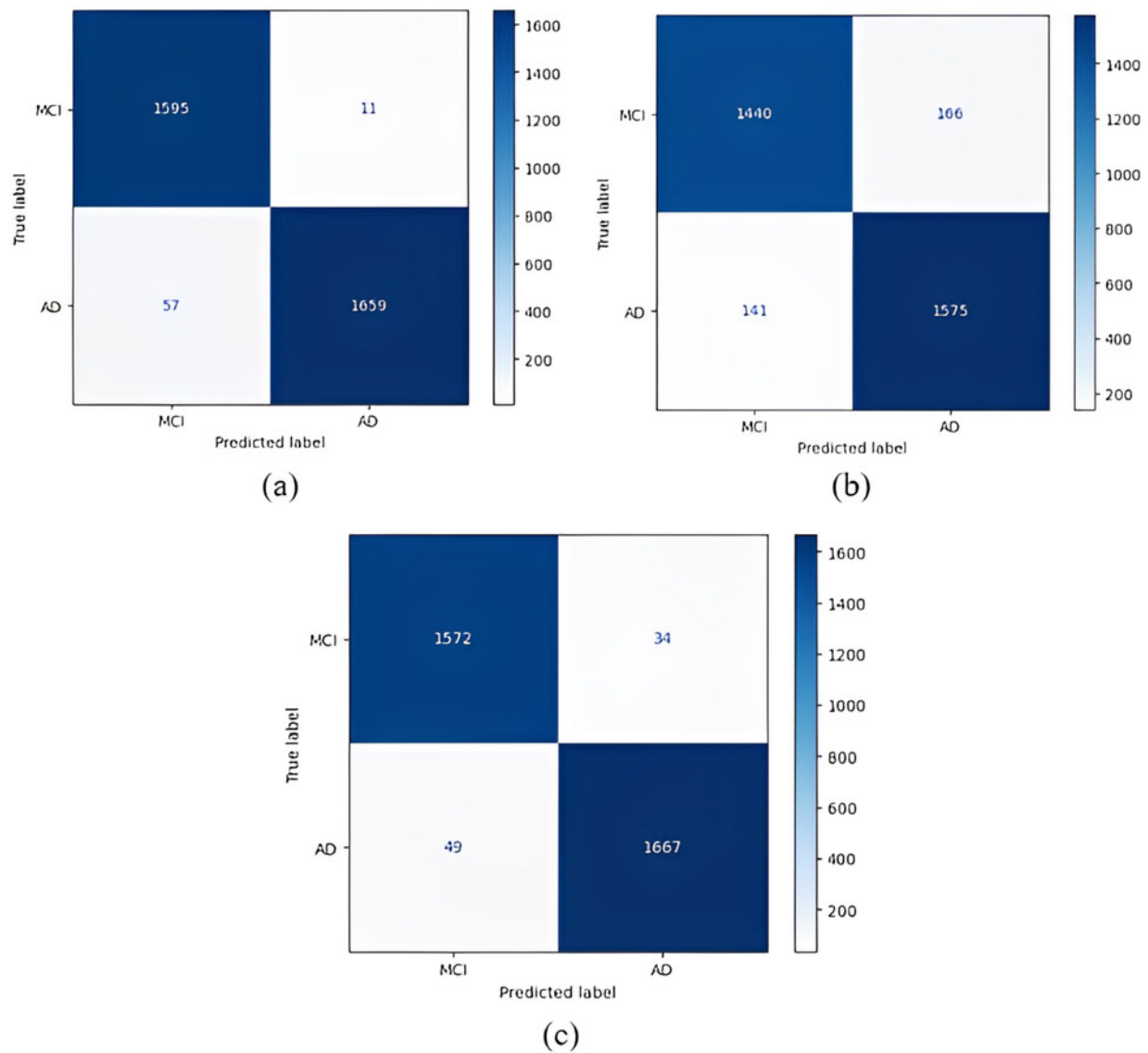


Figure 7

1 vs 1 classification confusion matrices (CN/MCI)

1 vs 1 classification confusion matrices (CN/MCI) for (A) EfficientNetB0 model (B) DenseNet121 model (C) AlexNet model

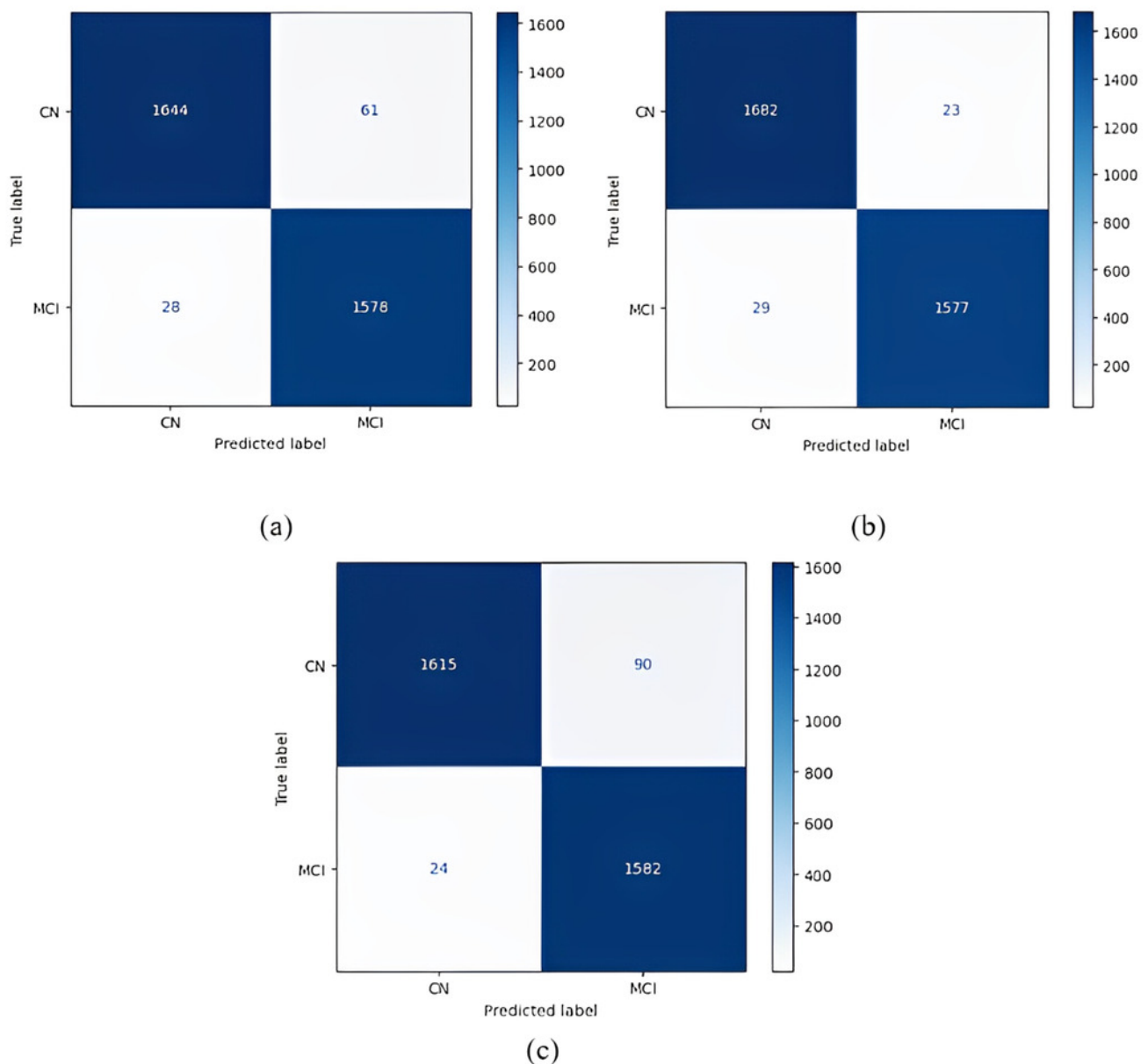


Figure 8

1 vs All classification confusion matrices (MCI/CNAD)

1 vs All classification confusion matrices (MCI/CNAD) for (A) EfficientNetB0 model (B) DenseNet121 model (C) AlexNet model

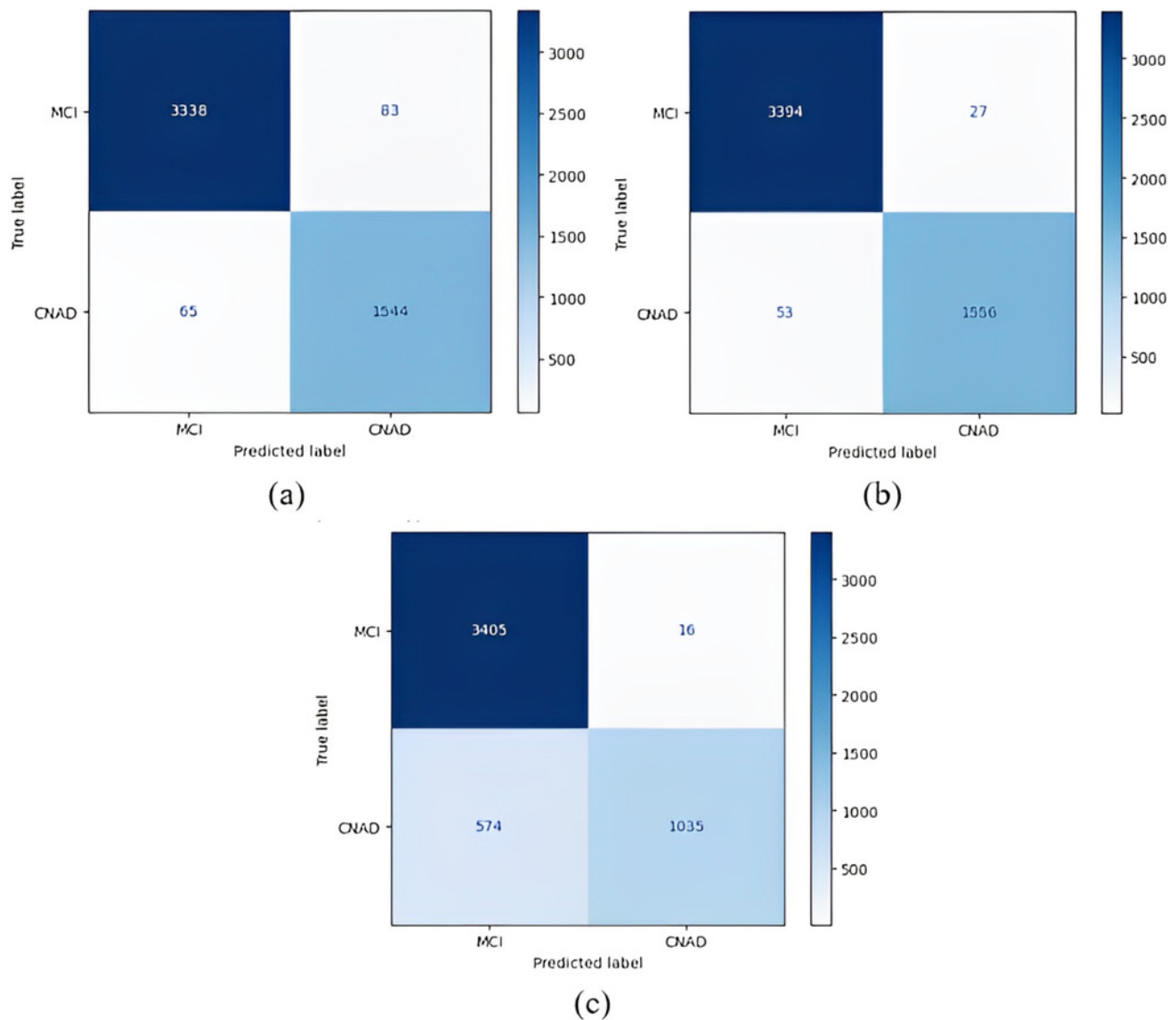


Figure 9

1 vs All classification confusion matrices (AD/CNMCI)

1 vs All classification confusion matrices (AD/CNMCI) for (A) EfficientNetB0 model (B) DenseNet121 model (C) AlexNet model

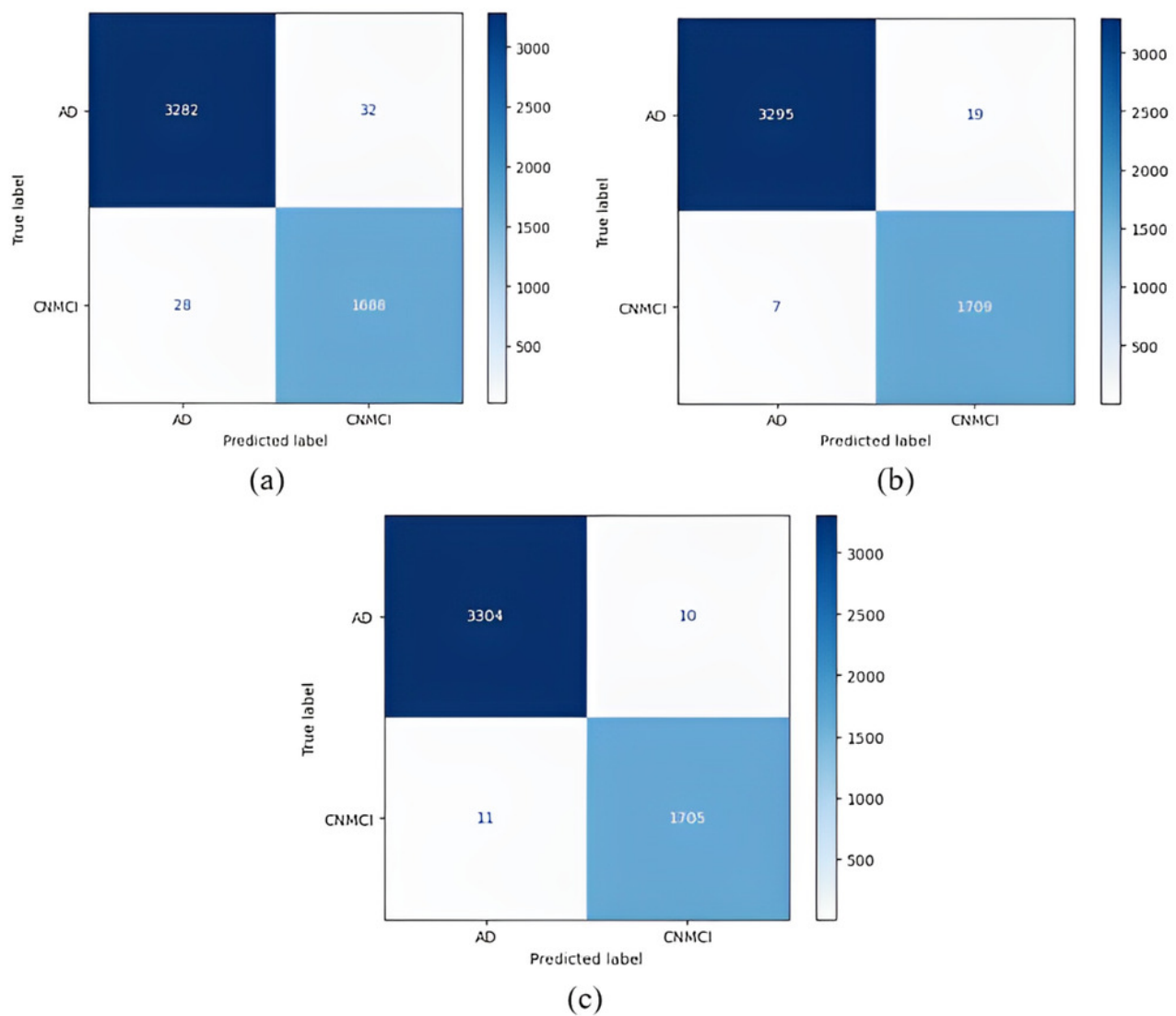


Figure 10

1 vs All classification confusion matrices (CN/MCIAD)

1 vs All classification confusion matrices (CN/MCIAD) for (A) EfficientNetB0 model (B) DenseNet121 model (C) AlexNet model

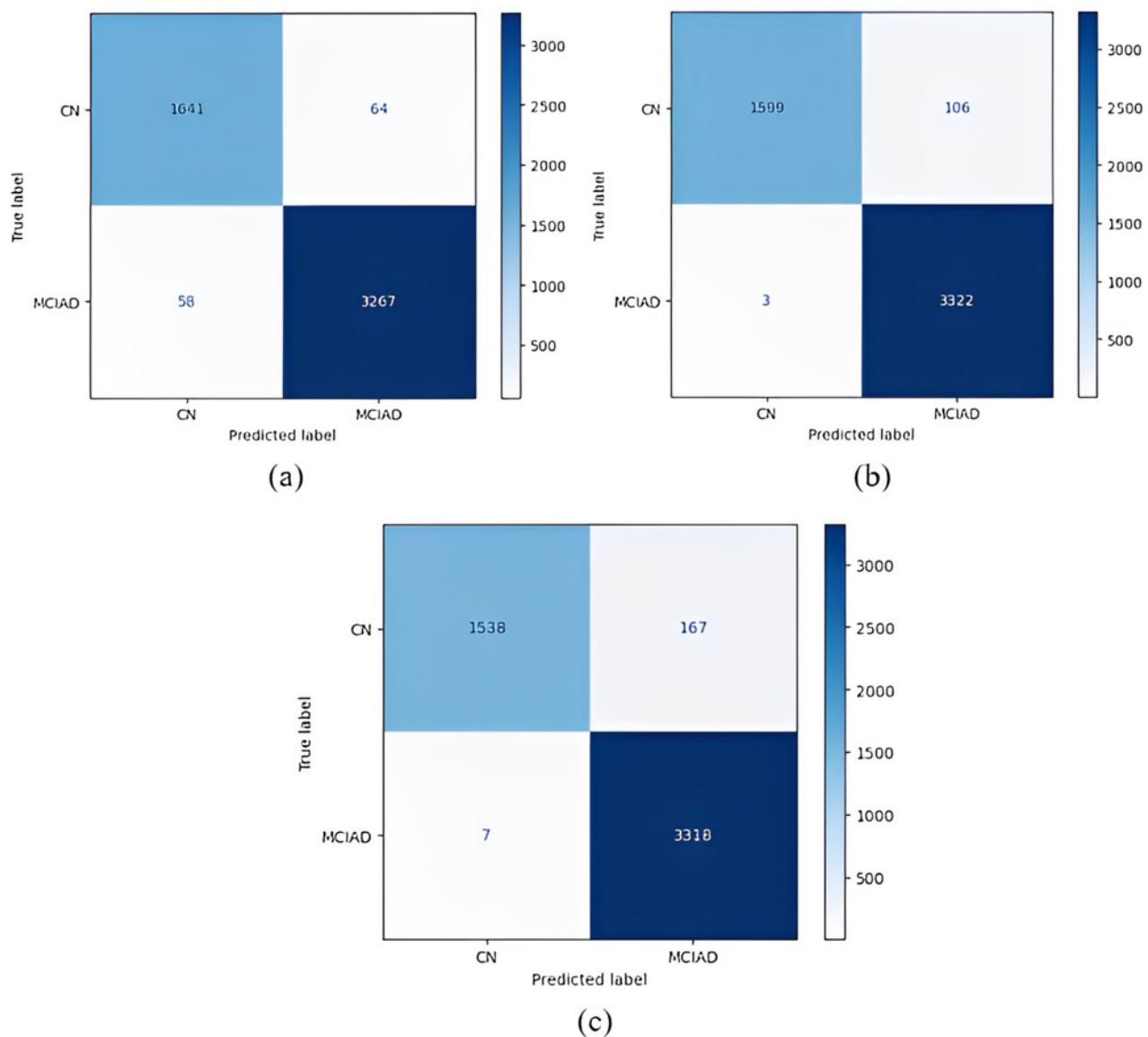


Table 1 (on next page)

The summary of the studies.

1

Table 1. The summary of the studies.

Reference	Year	Dataset	Models	Classes	Accuracy %
Shanmugam et al.	2022	ADNI	AlexNet	CN	97.34%
				EMCI	97.51%
				LMCI	95.19%
				MCI	96.82%
				AD	94.08%
			ResNet-18	CN	98.88%
				EMCI	99.14%
				LMCI	98.88%
				MCI	98.71%
				AD	97.51%
			GoogleNet	CN	97.17%
				EMCI	98.28%
				LMCI	97.60%
				MCI	98.37%
				AD	96.39%
Mehmood et al.	2021	ADNI	CNN	CN vs. AD (Group A)	95.38%
				CN vs. AD (Group B)	98.73%
Mohammadjafari et al.	2021	ADNI-1	VGG-16	AD, CN	88.50%
			ResNet50		83.88%
			DenseNet121		94.75%
Sethi et al.	2022	ADNI	CNN	CN vs. AD	82.32%
			CNN+SVM		89.40%
Naz et al.	2021	ADNI	VGG-19	MCI vs. AD	99.27%
			VGG-16	CN vs. AD	98.89%
			AlexNet	CN vs. AD	91.38%
			VGG-16	MCI vs. CN	97.06%
Farooq et al.	2017	ADNI	AlexNet	AD, LMCI, MCI, CN	98.88%
			ResNet-18		98.01%
			ResNet-152		98.14%

Savaş	2022	ADNI	EfficientNetB0 EfficientNetB1	CN, MCI, AD	92.98% 91.91%
Li et al.	2017	ADNI	CNN_S3 CAE_S2 CAE_S3 CAE_S4 Hybrid	CN, AD	84.12% 82.24% 81.19% 76.17% 88.31%
Khan et al.	2022	ADNI	XGB + DT + SVM	CN, MCI, AD	95.75%
Mohi ud din dar et al.	2023	ADNI	CNN	CN, LMCI, EMCI, MCI, AD	96.22%
Mora-Rubio et al.	2023	ADNI, OASIS	DenseNet EfficientNet VIT Siamese	CN vs. MCI CN vs. AD CN vs. LMCI CN vs. EMCI	66.41% 89.02% 80.56% 67.19%

2

3

Table 2 (on next page)

Classes and total scan numbers of these classes are given

1

Table 2. Classes and total scan numbers of these classes are given.

Class	Subjects	Total Scans
AD	40	4230
MCI	140	5961
CN	335	6575

2

Table 3 (on next page)

Training results when models run

1

Table 3. Training results when models run.

Models	Accuracy	Precision	Recall	Auc	F1 Score	Validation Accuracy
EfficientNetB0	0.9920	0.9890	0.9883	0.9994	0.9886	0.9844
DenseNet121	0.9856	0.9791	0.9778	0.9977	0.9783	0.9858
AlexNet	0.9977	0.9965	0.9965	0.9996	0.9964	0.9573

2

Table 4(on next page)

Testing results when models run

1

Table 4. Testing results when models run.

Models	Accuracy	Precision	Recall	Auc	F1 Score	MCC
EfficientNetB0	0.9733	0.9736	0.9729	0.9733	0.9731	0.9599
DenseNet121	0.9819	0.9819	0.9818	0.9822	0.9819	0.9711
AlexNet	0.9413	0.9436	0.9398	0.9399	0.9403	0.9106

2

Table 5 (on next page)

Training results when models run

1

Table 5. Training results when models run.

1 vs. 1	Models	Accuracy	Precision	Recall	Auc	F1 Score	Validation Accuracy
CN/AD	EfficientNetB0	0.9990	0.9985	0.9985	0.9999	0.9984	0.9892
	DenseNet121	0.9959	0.9939	0.9939	0.9996	0.9938	0.9850
	AlexNet	0.9980	0.9970	0.9970	0.9999	0.9970	0.9896
MCI/AD	EfficientNetB0	0.9987	0.9980	0.9980	1.0000	0.9980	0.9828
	DenseNet121	0.9972	0.9958	0.9958	0.9999	0.9957	0.9406
	AlexNet	0.9958	0.9937	0.9937	0.9989	0.9937	0.9841
CN/MCI	EfficientNetB0	0.9975	0.9963	0.9963	0.9996	0.9963	0.9724
	DenseNet121	0.9869	0.9869	0.9869	0.9987	0.9968	0.9767
	AlexNet	0.9961	0.9942	0.9942	0.9986	0.9942	0.9702

2

Table 6 (on next page)

Testing results when models run

1

Table 6. Testing results when models run.

1 vs. 1	Models	Accuracy	Precision	Recall	Auc	F1 Score	MCC
CN/AD	EfficientNetB0	0.9894	0.9895	0.9895	0.9890	0.9895	0.9790
	DenseNet121	0.9716	0.9718	0.9716	0.9720	0.9716	0.9433
	AlexNet	0.9774	0.9783	0.9776	0.9780	0.9775	0.9558
MCI/AD	EfficientNetB0	0.9795	0.9795	0.9800	0.9800	0.9795	0.9594
	DenseNet121	0.9075	0.9077	0.9072	0.9070	0.9074	0.8149
	AlexNet	0.9750	0.9749	0.9751	0.9750	0.9750	0.9500
CN/MCI	EfficientNetB0	0.9731	0.9730	0.9734	0.9730	0.9731	0.9664
	DenseNet121	0.9842	0.9843	0.9842	0.9840	0.9843	0.9668
	AlexNet	0.9655	0.9661	0.9661	0.9660	0.9656	0.9311

2

3

Table 7 (on next page)

Training results when models run

1

Table 7. Training results when models run.

1 vs. All	Models	Accuracy	Precision	Recall	Auc	F1 Score	Validation Accuracy
MCI/CNAD	EfficientNetB0	0.9984	0.9976	0.9976	0.9998	0.9976	0.9790
	DenseNet121	0.9970	0.9970	0.9970	0.9999	0.9969	0.9796
	AlexNet	0.9969	0.9953	0.9953	0.9993	0.9953	0.9233
AD/CNMCI	EfficientNetB0	0.9929	0.9894	0.9894	0.9991	0.9893	0.9915
	DenseNet121	0.9983	0.9983	0.9983	0.9999	0.9982	0.9915
	AlexNet	0.9990	0.9985	0.9985	0.9999	0.9985	0.9972
CN/MCIAD	EfficientNetB0	0.9973	0.9959	0.9959	0.9998	0.9959	0.9807
	DenseNet121	0.9853	0.9853	0.9853	0.9980	0.9852	0.9702
	AlexNet	0.9988	0.9982	0.9982	0.9999	0.9982	0.9776

2

3

Table 8 (on next page)

Testing results when models run

1

Table 8. Testing results when models run.

1 vs. All	Models	Accuracy	Precision	Recall	Auc	F1 Score	MCC
MCI/CNAD	EfficientNetB0	0.9705	0.9649	0.9677	0.9680	0.9663	0.9326
	DenseNet121	0.9840	0.9838	0.9796	0.9800	0.9816	0.9633
	AlexNet	0.8827	0.9203	0.8193	0.8190	0.8492	0.7362
AD/CNMCI	EfficientNetB0	0.9880	0.9865	0.9870	0.9870	0.9867	0.9734
	DenseNet121	0.9948	0.9934	0.9951	0.9950	0.9943	0.9885
	AlexNet	0.9958	0.9954	0.9953	0.9950	0.9954	0.9874
CN/MCIAD	EfficientNetB0	0.9757	0.9733	0.9725	0.9730	0.9729	0.9458
	DenseNet121	0.9783	0.9836	0.9685	0.9680	0.9754	0.9665
	AlexNet	0.9654	0.9738	0.9500	0.9500	0.9605	0.9234

2

Table 9 (on next page)

Possible outcomes of two classifiers

1

Table 9. Possible outcomes of two classifiers.

	Classifier A Failed	Classifier A Succeeded
Classifier B Failed	N_{ff}	N_{sf}
Classifier B Succeeded	N_{fs}	N_{ss}

2

3

Table 10(on next page)

z scores and confidence levels

1

Table 10. z scores and confidence levels.

z score	One-tailed prediction	Two-tailed prediction
1.345	95%	90%
1.960	97.5%	95%
2.326	99%	98%
2.576	99.5%	99%

2

3

Table 11(on next page)

z scores of architectures on Alzheimer's disease prediction

1

2

Table 11. z scores of architectures on Alzheimer's disease prediction for 1vs. 1.

1 vs. 1	CN vs. AD		
	EfficientNetB0	DenseNet121	AlexNet
EfficientNetB0	-	← 5.86	←4.44
DenseNet121	-	-	↑1.57
AlexNet	-	-	-
	CN vs. MCI		
	EfficientNetB0	DenseNet121	AlexNet
EfficientNetB0	-	↑ 3.66	←1.94
DenseNet121	-	-	←5.23
AlexNet	-	-	-
	MCI vs. AD		
	EfficientNetB0	DenseNet121	AlexNet
EfficientNetB0	-	←13.00	←1.31
DenseNet121	-	-	↑11.99
AlexNet	-	-	-

3

4

Table 12(on next page)

z scores of architectures on Alzheimer's disease prediction

1

Table 12. z scores of architectures on Alzheimer's disease prediction for 1 vs. All.

1 vs. All	CN vs. MCIAD		
	EfficientNetB0	DenseNet121	AlexNet
EfficientNetB0	-	↑0.86	← 3.41
DenseNet121	-	-	← 5.87
AlexNet	-	-	-
	MCI vs. CNAD		
	EfficientNetB0	DenseNet121	AlexNet
EfficientNetB0	-	↑ 4.94	← 17.46
DenseNet121	-	-	← 21.36
AlexNet	-	-	-
	AD vs. CNMCI		
	EfficientNetB0	DenseNet121	AlexNet
EfficientNetB0	-	↑ 3.84	↑ 4.87
DenseNet121	-	-	↑0.70
AlexNet	-	-	-

2

3